A TRIDENT SCHOLAR
PROJECT REPORT

NO. 258

Turnable Laser Light Source

UNITED STATES NAVAL ACADEMY
ANNAPOLIS, MARYLAND

19990121 132
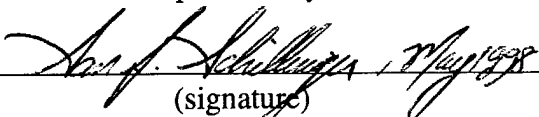
REPORT DOCUMENTATION PAGE

Form Approved
OMB no. 0704-0188

Public reporting burden for this collection of information is estimated to average 1 hour per response, including the time for reviewing instructions, searching existing data sources, gathering and maintaining the data needed, and completing and reviewing the collection of information. Send comments regarding this burden estimate or any other aspect of this collection of information, including suggestions for reducing this burden, to Washington Headquarters Services, Directorate for Information Operations and Reports, 1215 Jefferson

1. AGENCY USE ONLY (Leave blank)	2. REPORT DATE	3. REPORT TYPE AND DATES COVERED

4. TITLE AND SUBTITLE Tunable laser light source

5. FUNDING NUMBERS

6. AUTHOR(S)

Ian J. Schillinger

7. PERFORMING ORGANIZATIONS NAME(S) AND ADDRESS(ES)

U.S. Naval Academy, Annapolis, MD

8. PERFORMING ORGANIZATION REPORT NUMBER USNA Trident report; no. 258 (1998)

9. SPONSORING/MONITORING AGENCY NAME(S) AND ADDRESS(ES)

10. SPONSORING/MONITORING AGENCY REPORT NUMBER

11. SUPPLEMENTARY NOTES

Accepted by the U.S. Trident Scholar Committee

12a. DISTRIBUTION/AVAILABILITY STATEMENT

This document has been approved for public release; its distribution is UNLIMITED.

12b. DISTRIBUTION CODE

13. ABSTRACT (Maximum 200 words) A laser diode and a fiber Bragg grating can be used to construct a tunable laser light source. This new tunable laser has a central wavelength of 682.6nm (red light) and a bandwidth less than one twentieth of one nanometer. It is tunable over a range greater than five nanometers.

Tunable light sources have applications in fundamental research such as noise studies in optical amplifiers and high precision spectroscopy, as well as applications in optical engineering, including communications and LIDAR systems. Although tunable lasers exist for these purposes now, this new tunable laser has an unique construction. It contains a laser diode, which is a semiconductor pn junction diode that emits coherent light once a sufficient drive current is supplied, and an in-fiber Bragg grating that is used to modify the output of the laser diode. The grating provides additional feedback to the laser diode at the wavelength of the grating's Bragg condition. The combined system lases at this wavelength. Tuning is accomplished by straining the grating within its fiber and thus changing the wavelength of its Bragg condition. This strain is evolved by embedding the grating in a composite beam and deflecting the beam.

14. SUBJECT TERMS

Laser, Bragg, Grating

15. NUMBER OF PAGES

16. PRICE CODE

17. SECURITY CLASSIFICATION OF REPORT	18. SECURITY CLASSIFICATION OF THIS PAGE	19. SECURITY CLASSIFICATION OF ABSTRACT	20. LIMITATATION OF ABSTRACT

NSN 7540-01-280-5500

Standard Form 298 (Rev.2-89)
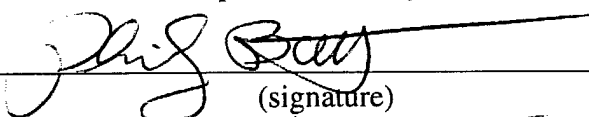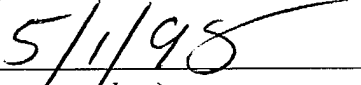
TUNABLE LASER LIGHT SOURCE

by

Midshipman Ian J. Schillinger, Class of 1998
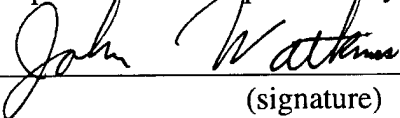United States Naval Academy
Annapolis, Maryland
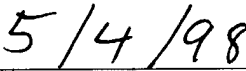
_____
(signature)

Certification of Advisers' Approval

Assistant Professor Philip R. Battle
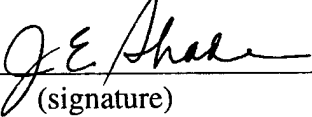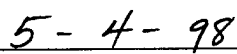Department of Physics

_____
(signature)

_____
(date)

Assistant Professor John M. Watkins
Department of Weapons and Systems Engineering

_____
(signature)

_____
(date)

Acceptance for the Trident Scholar Committee

Professor Joyce E. Shade
Chair, Trident Scholar Committee

_____
(signature)

_____
(date)

USNA-1531-2

Table of Contents

1.0.0 Abstract

A laser diode and a fiber Bragg grating can be used to construct a tunable laser light source. This new tunable laser has a central wavelength of 682.6nm (red light) and a bandwidth less than one twentieth of one nanometer. It is tunable over a range greater than five nanometers.

Tunable light sources have applications in fundamental research such as noise studies in optical amplifiers and high precision spectroscopy, as well as applications in optical engineering, including communications and LIDAR systems. Although tunable lasers exist for these purposes now, this new tunable laser has a unique construction. It contains a laser diode, which is a semiconductor pn junction diode that emits coherent light once a sufficient drive current is supplied, and an in-fiber Bragg grating that is used to modify the output of the laser diode. The grating provides additional feedback to the laser diode at the wavelength of the grating's Bragg condition. The combined system lases at this wavelength. Tuning is accomplished by straining the grating within its fiber and thus changing the wavelength of its Bragg condition. This strain is evolved by embedding the grating in a composite beam and deflecting the beam.

Keywords: Laser, Bragg, Grating.

2.0.0 Introduction

In this research, a tunable laser was constructed using a laser diode and a special optical fiber. The wavelength of the output is tunable over a range of five nanometers centered at a wavelength of 683 nanometers. Lasers which are tunable have been constructed before. However, in contrast to traditional tunable lasers, the feedback mechanism in this optical source is embedded within an optical fiber. Furthermore, because a diode laser and an optical fiber have been used, this optical source can be more compact and robust than traditional designs.

The construction and characterization of a tunable laser is somewhat analogous to the development of superheterodynes in FM radios. These circuits listen to distant radio broadcasts, decoding information by comparing what they hear to an internal, stable, tunable electronic signal. When this internal signal is very narrow, the radio will have good channel resolution. The farther the radio can be tuned, the more channels are available to it. Without this native signal, the radio loses these pleasing characteristics.

Good filtering and a wide range of tunability are characteristics which we have come to expect from modern radios, and filtering and tunability are the primary objectives of this research. Good filtering will give the laser a narrow bandwidth. Bandwidth is the range of frequencies in the laser output. Tunability implies that the wavelength of the output can be varied, depending upon the requirements of the application.

A narrow-band, tunable laser has many applications in optical communications and fundamental research areas such as spectroscopy. Optical communications require many channels to be useful and each channel must be narrow in order to prevent overlapping with adjacent channels. In the FM example, a narrow band source within the radio provides very fine resolution of channels. A narrow band, laser light source such as the one in this research could fill a similar role in an optical communication system. Tunability is important because it allows "dialing" among the available channels. Spectroscopy can also benefit from a tunable laser, since the composition of materials can be determined by their absorption spectra. A narrow-band laser would be able to

distinguish between closely related materials, and tunability would make the laser useful for many different substances.[1]

  In order to describe the research behind the optical source, some background information will follow directly. After that, the experiments supporting this research will be described and the results will be discussed. Interpretations of the results are offered in a summary at the end and these are followed by the appendices. The researchers acknowledge the very generous assistance of the men and women of the U. S. Naval Academy faculty and staff.

3.0.0 Acknowledgements:

4.0.0 Background

The background of the tunable laser must begin with a discussion of the laser. LASER stands for: **L**ight **A**mplification by **S**timulated **E**mission of **R**adiation. A laser usually consists of an optically active medium--that is, something which can be excited to emit light--and a surrounding pair of mirrors. As shown in Figure (1), light from the medium is emitted in all directions and some of it is redirected by the mirrors, back through the medium. When this reflected light reenters the medium, it is copied, or amplified. This amplified light reemerges from the medium and once again is redirected by the facing mirror. In this way, a cycle of light reflections and amplifications begins. Because of this cycle of amplification, furthermore, the output of a laser is coherent. Coherent light is uniform in wavelength and phase. All of the waves are the same length and their peaks and valleys line up as they travel through space.[2]

A very important point is that, while the medium may emit light over a broad bandwidth, only certain frequencies are allowed to resonate, or stand, in the laser cavity. As the light cycles between the two mirrors, certain wavelengths interfere constructively. They persist in the cavity because of this constructive interference. Figure (1) shows that, in order for a wavelength to interfere constructively with itself in a laser cavity, an integral multiple of its half-wavelength must equal the cavity length. These allowed wavelengths are called "modes" of the laser cavity.[3] As shown in Figure (2), where the laser is modelled as a dynamic system, this resonance condition acts as a filter, limiting the output of the laser to those wavelengths that intersect the laser gain profile (Figure (2b)) and the cavity resonance condition (Figure (2c)).

The mirrors surrounding the optical medium in a laser act as feedback elements. Because the mirrors are only partially reflective, a portion of the light inside the laser is fed back into the laser process and the rest constitutes the output. In this research, the output of the laser is coupled into an optical fiber that contains a Bragg grating. As we will describe next, and as shown in Figure (3), this grating functions as an additional mirror, causing more feedback to the active medium, and further refining the output of the combined system.

Optical fibers are thin filaments of glass which "conduct" light much as wires conduct electricity. A fiber which contains a Bragg grating is a special fiber with a periodic variation of its density. Bragg gratings are like windows in a lighted room when it is dark outside. Light is transmitted through the windows, since we know that an observer outside will see into the room. At the same time, a reflection of things in the room can be observed in the window pane from within. This is so because light is reflected by the change in density from air to glass as it leaves the room through the window. As Figure (4) shows, a Bragg grating contains many of these index changes. Instead of shifting from air to glass, however, these changes shift from higher to lower index fiber material. As light travels through the grating, there are many back-reflections. Some of the light escapes to the right through the grating, and this constitutes the total system output. Approximately fifty percent of the light is returned to the left, however, and will be fed back to the active medium where it will be amplified. The wavelength of this feedback is determined by the spacing of the grating surfaces. The grating separation is equal to one half of the wavelength which will interfere constructively upon reflection. All other wavelengths will interfere destructively in the feedback path and will therefore be attenuated--that is, they will not survive to be amplified in the diode medium.[4]

An important property of the Bragg grating is its tunability. The reflected light rays in the grating will line up if the distance between the density changes is an integral multiple of one half of the wavelength of the rays. This implies that changing the spacing of the density variations causes the reflected wavelength to change. This is tuning. As shown in Figure (5), when the grating is compressed, the spaces in it become smaller and the waves resonating in it will have smaller wavelengths. When the grating is extended, the spaces in it become larger and it will support larger wavelengths.[5]

Finally, as implied above, the combination of the laser and the fiber grating creates a dynamic system. Light coming from the optical medium is injected into the

fiber grating, and the grating creates feedback and allows for the possibility of controlling the wavelength of the feedback. Figure (3) shows the block diagram for the tunable laser. In it, the gain medium generates light while the diode cavity and the fiber grating filter the light. The filtered light returns to the diode, where it can stimulate the emission of like wavelengths, and thus be amplified. Light coming from the diode and heading to the grating is the "feed-forward" and is supplied by aligning the diode emissions with an optical fiber. The process of returning light to the amplifying material is called "feed-back" and this occurs through the reflective behavior of the grating as discussed above. The continuous flow of light constitutes a signal within a closed-loop optical system. In its steady state, the system selects modes according to the combined filter functions of the grating and the diode cavity. The system resonates at these wavelengths in steady state. Figures (3d) and (3e) illustrate that, by adjusting the grating dimensions to pass only one of the diode modes, a narrow-band, tunable output is obtained.

5.0.0 Experimental Setup

In the first phase of this research, the laser diode was characterized by analyzing its output power, bandwidth, and frequency. In the second phase, the grating was added to the overall system and the effects of this change were investigated. The setup used for the first phase is shown in Figure (6). Notice that the fiber grating was not yet a part of the experiment. The laser diode in the diagram is a GaAs, pn-junction diode. The Helium-Neon (HeNe) lasers in Figure (6) were used for calibrating the system because they have specific, known wavelengths. A green laser was used at 543.5 nm, an orange laser at 594.5 nm, and a red laser at 632.8 nm. The light from these laser sources was focused into optical fibers that were coupled to a spectrometer. The light from the HeNe lasers was focused with converging lenses. In the case of the diode laser, however, the output was elliptical and the multiplication of optical components necessary to inject the light into an optical fiber lead to unwanted feedback into the diode laser. Therefore, light was coupled from the diode by positioning the fiber

terminus as close to the diode laser output surface as possible. In order to maximize the light injected into the fiber, considerable time was spent to position the fiber in precise relation to the diode beam. Micropositioning stages were used to brace and maneuver the fiber tip until it was located near the point of emission on the diode surface.

Figure (7) shows that the spectrometer spread light that passed through it into a spectrum, spatially separating the various wavelengths. This spectrum was detected by an array of 1024 charge-coupled devices (CCD array), which are very small, light-sensitive electronic elements. The sensors were arranged in a line along the wavelength axis of the spectrometer output. When light from the spectrometer illuminated one of these elements, the circuit began to collect an electrical charge. The array was scanned by a computer once every 28 milliseconds. The scanning read and reset each element in order and showed the charge variations along the array as a line on an oscilloscope. Thus a digital image of the spectrometer output was displayed on an oscilloscope. Figure (7) shows the relationship between the input to the spectrometer and the output of the oscilloscope. Note that the output of the spectrometer was digitized by the CCD array. This is an important consideration below, where the resolution of the spectrometer and CCD array is investigated. Finally, as shown in the experimental setup, Figure (6), the information gathered by the array was stored on a computer.

5.1.0 Spectrometer

The spectrometer was the center of the sensor setup. A spectrometer, as shown in Figure (8), produces the spectrum of the light passing through it by spreading the light into component wavelengths. Most light sources (such as incandescent light bulbs) emit light over a broad spectrum. Lasers, because they emit light at specific wavelengths, show up as very narrow, bright lines. A spectrometer's output is displayed as a plot of intensity of light versus wavelength. The spectrometer has two major characteristics--dispersion and resolution. The spectrometer used in this research was a

Jarrel-Ash Monospec 27. The Monospec 27 is a Czerny-Turner configured spectrometer, as shown in Figure (8). The grating used in the spectrometer was a plane, reflective grating with 600 grooves per millimeter.

5.1.1 Dispersion

Dispersion is a measure of the separation between individual wavelengths in the spectrometer output. As shown in Figure (9), large dispersion will enlarge the wavelength axis, stretching a spectrum out more, while narrow dispersion will display wavelengths closer together on the abscissa. Dispersion, then, determines the scale of the wavelength axis. As Figure (10) shows, incoming light rays are reflected by a grating that is internal to the spectrometer. These reflected light rays diffract and spread into one another. When the path difference between similar reflected rays is an integral multiple of their wavelength, they interfere constructively and a bright line appears at the spectrometer output. Different wavelengths will interfere constructively at different angles from the grating normal. Thus a spectrum of wavelengths exists in an arc from the normal of the grating. Also, since the grating condition is periodic, the spectrum is repeated. Each repetition is called an *order* of the original image. Given the wavelengths involved and the spectrometer's mechanical limitations, the highest observable order in the spectrometer was the third order. As shown in Appendix A, the grating condition in Figure (10) can be used to convert the spectrometer output to a wavelength--this scaling conversion factor is the dispersion.[6]

The dispersion of this spectrometer was measured in the first three orders. To do this, the procedure outlined below, and discussed in detail in Appendix A, was followed.

1. Three different HeNe lasers were injected into the spectrometer simultaneously. The wavelengths of the lasers were : (1) 632.8 nm; (2) 594.5 nm; (3) 543.5 nm.

2.   In each order, the time delay between the bright lines on the oscilloscope display of the spectrometer output was measured.

3.   The time delay on the oscilloscope was converted to a distance on the CCD array.

4.   That distance was compared to the "known wavelength" separation of the bright lines and thus an expression for the dispersion was found.

The results of these measurements are shown in Table I and again in Appendix A. As shown there, they agree closely with the theoretical predictions for dispersion in each order.

Table I -- Predicted and Measured Dispersions

Order	Predicted	Measured
1	5.8 nm/mm	5.72 nm/mm
2	2.6 nm/mm	2.59 nm/mm
3	1.5 nm/mm	1.50 nm/mm

5.1.2 Resolution

The second telling characteristic of the spectrometer is its resolution, which is discussed in detail in Appendix B. As shown in Figure (11), a spectrometer with good resolution will display the single wavelength of a laser as a sharp, bright image. A spectrometer with poor resolution will display the same line with considerable spreading of the image, similar to a camera out of focus.[7] It is important to note that the resolution of the spectrometer was further conditioned by the digital nature of the CCD array, so that the measured resolution was a convolution of spectrometer and CCD array resolutions. In the third order, for example, the pixel size of the CCD array corresponded to 0.4 Angstroms (Appendix B). As a result, the wavelength axis of the data was limited to 0.4 Angstrom divisions and any data finer than this were observed

as a 0.4 Angstrom-wide region of brightness on the oscilloscope.

With this in mind, the resolution of the spectrometer/CCD array was evaluated using one of the HeNe lasers. A Helium-Neon laser has a very small bandwidth (virtually a delta function), so that the width of its image in the spectrometer output was due to the resolution of the spectrometer. As shown in Appendix B, a third-order image width of 0.06 Angstroms, or 0.006 nanometers, was expected for the red HeNe laser (632.8 nm). This prediction, however, was modified in light of the CCD pixel size, which in third order was 0.4 Angstroms. In Figure (12), a plot of image width versus image position on the CCD array is shown for the HeNe laser. As the plot shows, there is a region in the output field, between CCD elements 400 and 500, where the resolution is as good as we expected: one CCD element wide. The plot of image widths also shows that the resolution is much worse on the fringes of the array. The spreading was determined to be a geometric consequence of substituting a long CCD array for a narrow output slit. The spectrometer used is a Czerny-Turner configuration, which normally has an output slit to limit the field of view. Figure (13) shows how the optics of the spectrometer are aligned to provide optimum focus at the location of the output slit. The image width plot shows that, on the CCD array, the region of optimum focus is located where the output slit would have been (output center). However, the focus deteriorates rapidly to the left and right of the slit because of the internal geometry of the spectrometer. To the left of the center, the focus occurs before the array. To the right of the center, the focus occurs behind the array. Due to these focus variations, measurements requiring fine resolution were made in the region of optimum focus--i.e., the center of the CCD array.

In summary, the resolution depended upon the spectrometer's natural spreading action, the digital nature of the sensors, and the focus at the output array. The primary purpose of analyzing the resolution was to determine if it was sufficient for this research. That is, the resolution of the sensor suite was sufficient if it resolved the details (harmonic mode structure) of the laser diode spectrum. The modes of the laser diode were separated by approximately two and one half Angstroms. As shown in

Figure (14), data collected from the laser diode in the third order of the spectrometer clearly display this mode structure of the diode , as well as the digital nature of the CCD array.

6.0.0 Laser Diode

With the experimental setup characterized, construction of the tunable laser began. This required its two major components--the laser diode and the fiber grating-- to be tested and assembled. The first of these was a GaAs pn-junction laser diode which emitted light when a current was driven through it. It differed from a normal laser in some important ways. First, the laser diode has a broad spectrum (about 10 nanometers). It can emit light composed of many wavelengths. Each of these wavelengths is called a *mode* of the diode laser. At low currents they are emitted simultaneously. Figure (14) shows the modes in a portion of the diode spectrum as they were observed by our spectrometer and CCD array. Recall that these modes are the wavelengths which resonate in the diode cavity.[8]

Second, as the power input to a laser diode increases, its output becomes *single-mode*, which is to say that only one of the diode's modes will predominate and the others will give their energy to that single mode. Figures (15), (16), and (17) show the diode spectrum observed at some points in the transition from the multi-mode state to the near-single-mode state. This threshold occurs at a drive current of approximately thirty milliamperes for this diode. The transition occurs as the gain curve narrows and selects one mode from the diode cavity mode structure.[9]

Finally, as the power continues to increase, higher modes will be selected and the output wavelength switches to these. As the laser diode redshifts, higher modes fall under the gain curve and lower modes fall out of it. The shift in the gain curve occurs because of electronic structure changes in the gain medium at higher drive currents.[10] The output remains single-mode. The spectrum shown in figure (18) was taken from the diode as this occurred.

Figure (19) shows the laser diode output power as a function of the drive

current. These data exhibit a threshold in the vicinity of thirty milliamperes--the threshold current. The laser region was characterized by a steeper slope between the drive current and the output power than the multimode region. As the figure shows, the diode assumed its laser character very suddenly around thirty milliamperes.

Figure (20) shows the laser diode bandwidth as a function of the drive current. As the current increased, the bandwidth of the output narrowed, especially in the transition from the multimode state to the single-mode state. These data can also be used to locate the laser state. Here again, the transition occurred in the vicinity of thirty milliamperes, which correlates with the threshold observed in Figure (19).

Figure (21) shows the output central wavelength with respect to the drive current. Here again, there was a threshold at thirty milliamperes which can be used to locate the laser state. Once the diode was in its laser state, successively higher modes were selected from the diode's broad comb of modes. As Figure (21) shows, the central wavelength of the laser diode drifted approximately one nanometer higher per ten milliampere increase in drive current.

7.0.0 Fiber Bragg Grating

With the diode installed and characterized, the first components of the light source were in place. What remained, then, was to inject the light from the diode into the fiber grating and observe the new behavior of the combined system. The experimental setup was modified as shown in Figure (22). Coupling the grating was a two-fold process: the fiber with the grating was mated with the diode output, providing additional, filtered feedback to the laser diode; then the spectral results of this change were investigated.

To mate the fiber grating to the laser diode, the fiber containing the grating was positioned very near to the diode output facet. To couple the fiber to the laser diode, the fiber end had to be cleaved very smoothly. It was then braced and adjusted with a micrometer stage until a maximum throughput was realized--about five milliwatts, or twenty percent of the maximum laser diode output power. Observations of the broadband output of the laser at a low power level showed that the grating was not yet feeding back enough light to start a laser reaction. As shown in Figure (23), the primary

effect of the grating at this power level was to filter out the characteristic wavelength of the Bragg grating from the broadband spectrum of the diode. The magnitude of this filtering function was seen in the depth of the dip in the otherwise Gaussian form of the diode spectrum. The grating feedback was about 50 to 60 percent of the magnitude of the diode spectrum at the grating wavelength. In its unstrained state, the wavelength of the grating feedback was found to be 682.6 nanometers, consistent with the manufacturer's specifications.

Installing the grating in the system had some remarkable effects. Spectra of the system with the grating installed are shown in Figures (24) and (25). First, the diode began to lase at significantly lower drive currents, about five to ten milliamperes below its uncoupled threshold. Figure (26) shows the output power curve of the combined system with the output power curve of the laser diode alone. In Figure (26), the new laser threshold of the combined system (Phase II) is five milliamperes below that of the laser diode alone (Phase I). The combined system also exhibits a steeper rate of increase in output power per increase in drive current. Each of these new characteristics was the result of the increased quantity of feedback. About half of the light which normally escaped the diode was returned by the grating. In being returned to the laser diode, the light was allowed to be amplified, leading to increased output for lower drive currents and greater increases in output power for each increase in drive current.

Second, when the diode moved into its single-mode regime, it did so at the Bragg wavelength of the grating. This occurred because the grating provided feedback to the optical medium at a very specific wavelength. As stated before, that wavelength was a characteristic of the spacing of the reflective index changes in the grating. Increasing the drive current increased the magnitude of the diode output and thus the amount of light incident upon the grating and the amount of light reflected by the grating. As the magnitude of this feedback increased, its effects began to predominate in the system. Since the feedback occurred at a very specific wavelength, the system output began to gravitate to that wavelength. Therefore, in the single mode regime, the single most important factor in the wavelength of the output of the system was the wavelength of the grating feedback. Figures (23), (24), and (25) show system spectra during the transition from broadband to narrow-band behavior. Note that, unlike the case of the laser diode alone, the output of the combined system remains locked to the

Bragg wavelength, independent of the drive current--i.e., there is no wavelength shift in the combined system.

7.1.0 Tuning

Finally, as noted in Section 1.0.0, the wavelength of the grating feedback was variable. In order to change the characteristic wavelength of the grating, the spacing of its reflective index changes had to be changed. This could be done most readily by applying a strain to the grating material. A tunable range of five nanometers was set as a goal, centered on the unstrained wavelength of the grating (682.6nm). Figure (27) shows how the grating was embedded in the top surface of a fiber glass beam as a preparation for straining the grating. As the layers of the beam were being layered, the grating containing the fiber was woven into the top layer of fiber glass. When the beam cured, the grating and fiber were a part of the top surface of the beam.

As shown in Figure (28), the top surface of the beam stretched when it was bent downward and thus the grating stretched with it. When the beam was deflected upward, the top surface of it was compressed, and with it the grating. The beam containing the grating was deflected over thirty different radii, and the wavelengths corresponding to these strains were observed with the spectrometer equipment. As figure (29) shows, the wavelength of the laser varied in direct proportion to the applied strain. The laser, as strained in the composite beam, was tunable over the five nanometers desired. Figure (30) shows some tuned states of the laser superimposed upon the broadband spectrum of the laser diode. Two issues limited the range of tunability. First, the laser was not tunable beyond the broadband gain curve of the laser diode as shown in the background of Figure (30). As the beam was bent upward and the wavelength of the laser moved lower, its output was observed to decrease as it went toward the left edge of the broadband curve of the diode. Although the Bragg condition of the grating was supporting these wavelengths, they were neither emitted nor amplified by the diode material. The second factor affecting the tuning range of the laser was the radius of curvature of the fiber glass beam. Specifically, the beam could only be bent so much before the resistance to further bending made further tuning infeasible. This defined the upper (highest wavelength) limit of tuning whereas the gain curve consideration defined

the lower (lowest wavelength) limit of tuning.

7.1.1 Continuity

Finally, the laser did not tune continuously over its entire range. Instead, the spectral output contained periodic gaps. These gaps occurred where the grating wavelength fell between two modes of the diode cavity as shown in Figures (3d) and (3e). In these cases, the wavelength selected by the grating was cancelled out by the filtering effects of the diode cavity. Figure (31) shows three adjacent tuned states of the laser. Note that these states are separated by 2.5 Angstroms, the diode cavity mode spacing.

8.0.0 Conclusion

In conclusion, this project investigated the possibility of constructing and characterizing a tunable light source from a laser diode and a fiber Bragg grating. During the research, just such a tunable laser was constructed. The laser, with the fiber grating embedded in a composite beam for tuning, has a central wavelength of 682.6 nanometers and a tunable range of five nanometers. Within this range, the system will only lase at the available modes of the laser diode and its output is, therefore, discrete.

The tunable laser can be described as a dynamic system. In that model, the laser diode provides a gain medium, a filter, and a feedback path. The fiber grating acts as an additional filter and provides another feedback path. The system is tuned by varying the fiber grating filter function (Bragg condition) and thus the wavelength of the light fed back to the laser diode.
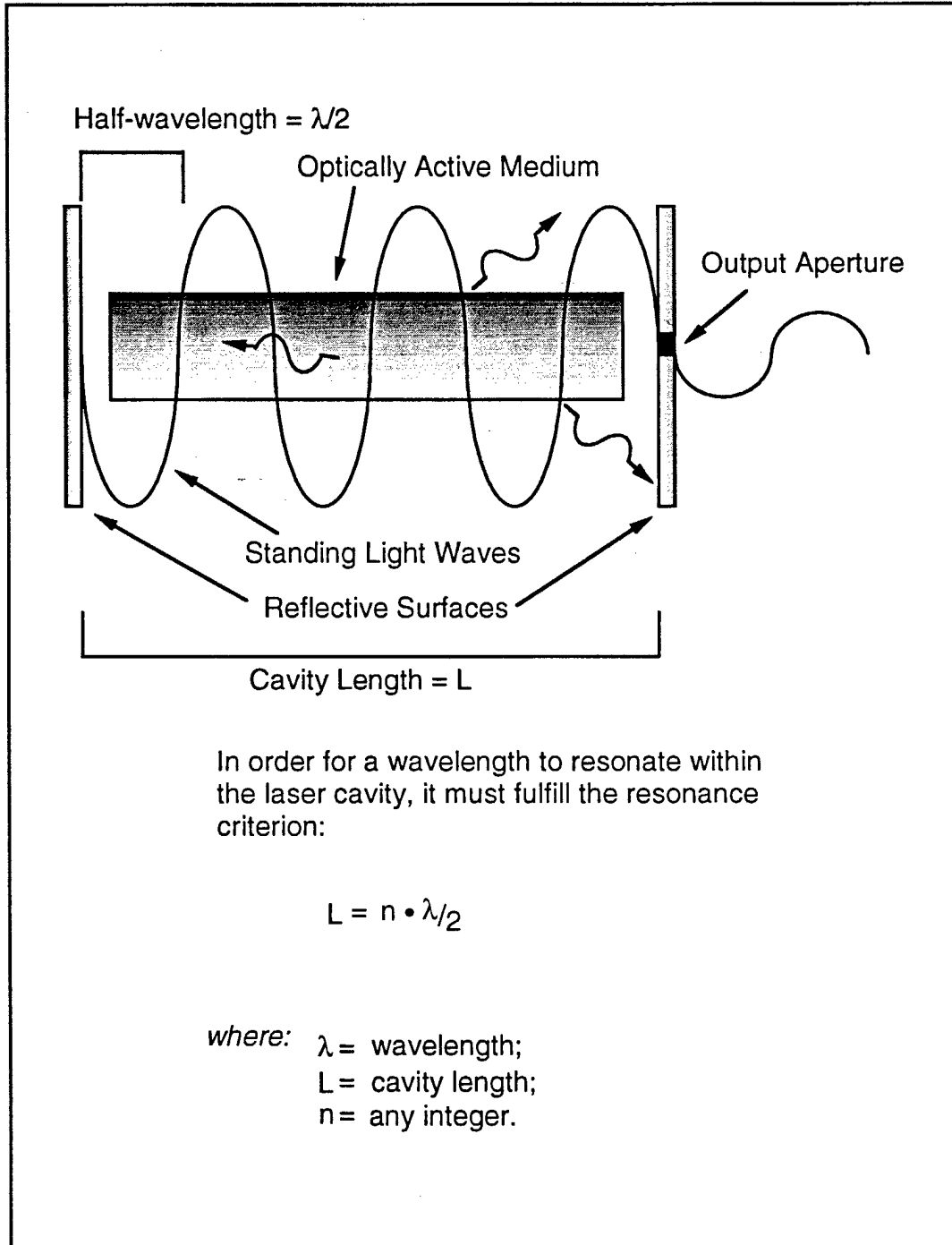
8.1.0 Future Work

Much can be done to refine the tunable laser. A more sophisticated tuning method would make the tunable laser more stable and controllable in its tuned states and could potentially reduce its size. A piezoelectric device or a nanopositioning motor might fulfill these expectations. Optical tuning methods using photoreactive materials

might also be used to change the Bragg condition of the grating with greater speed and accuracy.

In future experiments, the mode selection which interrupted the continuous tuning of the laser might be eliminated by coating the output facet of the laser diode with an antireflective coating. As a result, the diode cavity would lose some of its filtering ability and the wavelengths between its modes would not be lost. These and other such refinements could turn this tunable laser into a viable technology.

Laser Cavity Diagram

Half-wavelength = $\lambda/2$

Optically Active Medium

Output Aperture

Standing Light Waves

Reflective Surfaces

Cavity Length = L

In order for a wavelength to resonate within the laser cavity, it must fulfill the resonance criterion:

$$L = n \cdot \lambda/2$$

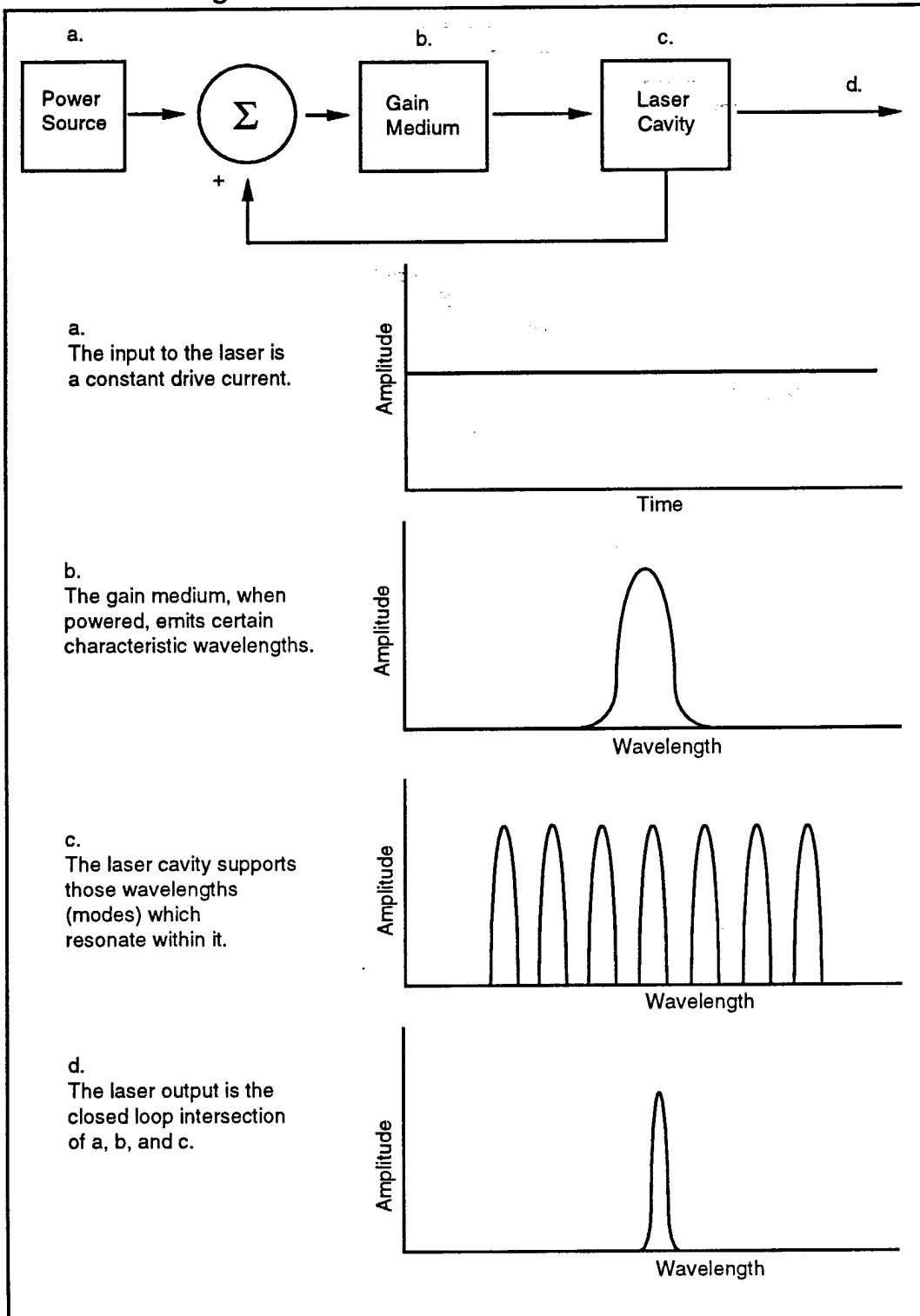*where:* λ = wavelength;
L = cavity length;
n = any integer.

The LASER consists of an optically active medum and a resonance chamber. Only those wavelengths whose half-wavelengths fit in the cavity an integral number of times will resonate.
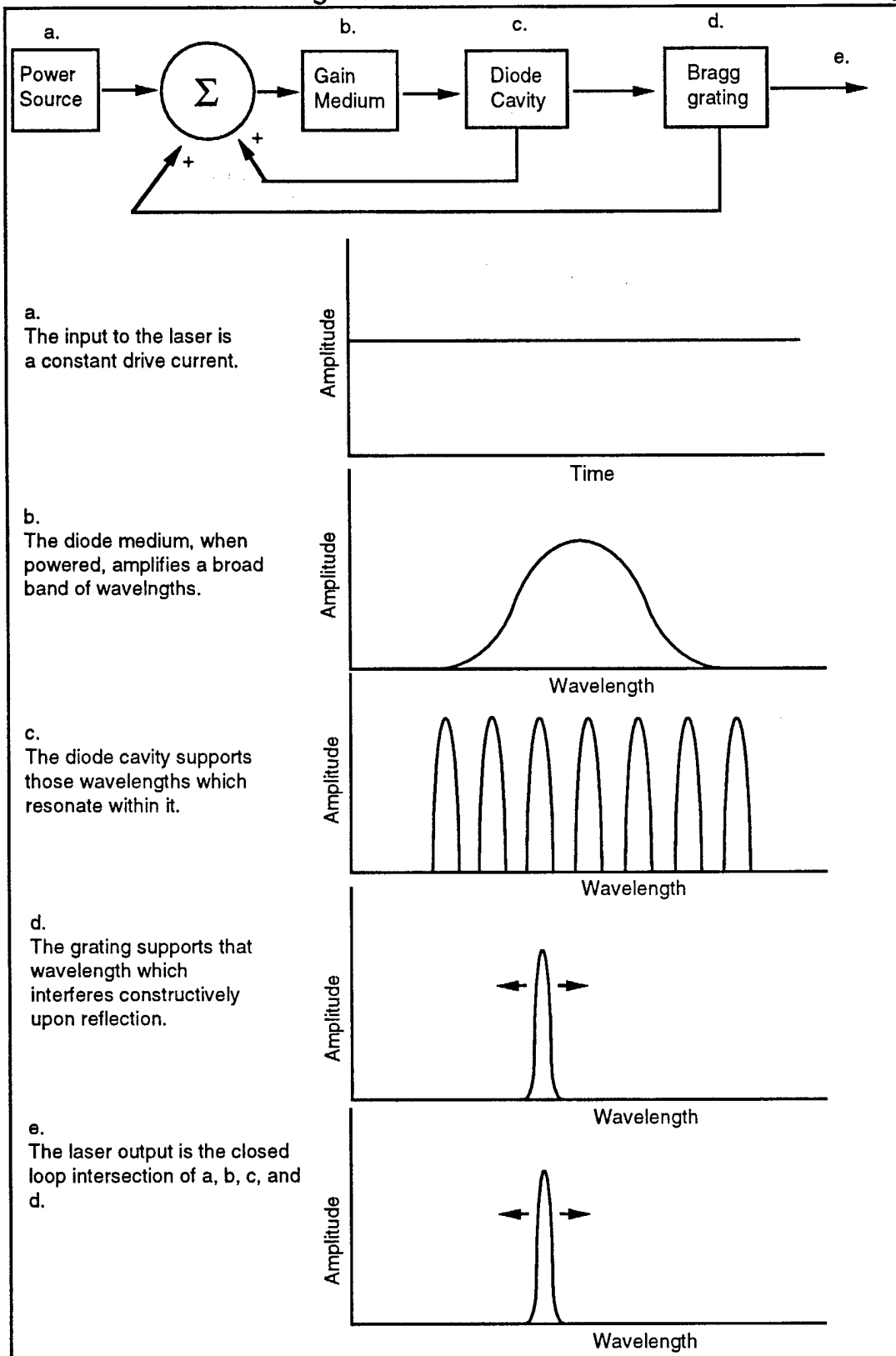
Figure 1

Laser Block Diagram

a. Power Source → Σ → b. Gain Medium → c. Laser Cavity → d.

a.
The input to the laser is a constant drive current.

b.
The gain medium, when powered, emits certain characteristic wavelengths.

c.
The laser cavity supports those wavelengths (modes) which resonate within it.

d.
The laser output is the closed loop intersection of a, b, and c.

The LASER is a dynamic system which uses feedback and filtering.

Figure 2

a.
The input to the laser is a constant drive current.

b.
The diode medium, when powered, amplifies a broad band of wavelngths.

c.
The diode cavity supports those wavelengths which resonate within it.

d.
The grating supports that wavelength which interferes constructively upon reflection.

e.
The laser output is the closed loop intersection of a, b, c, and d.

The tunable laser is a dual-feedback dynamic system.   Figure 3

Fiber Bragg Grating Diagram

Incident Light

Output Light

Feedback Light

Semi-Reflective Index Changes

The Fiber Bragg Grating is a **FILTER** and a **FEEDBACK MECHANISM**

Incident Light

Amplitude

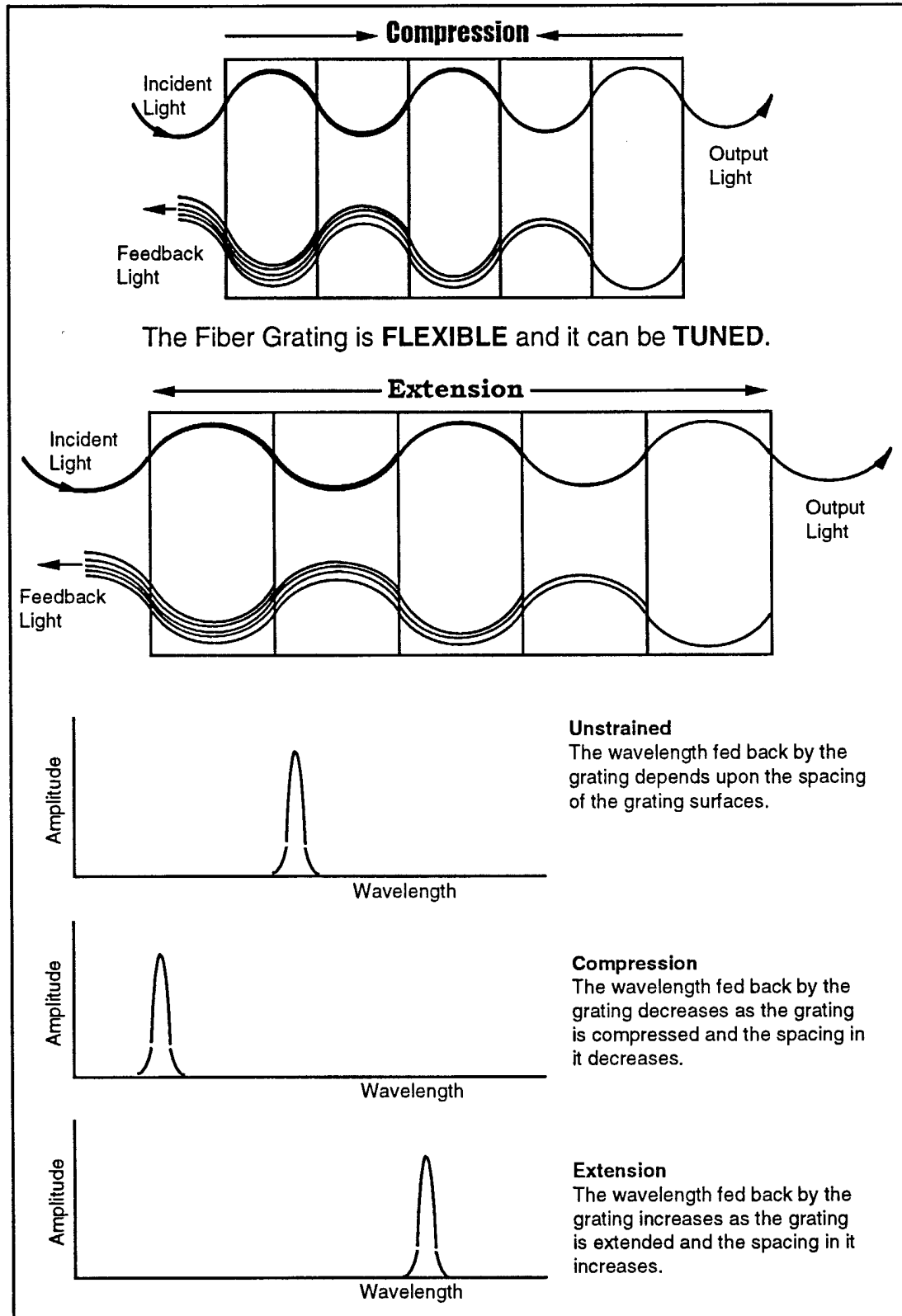Wavelength

Feedback Light

Amplitude

Wavelength

Output Light

Amplitude
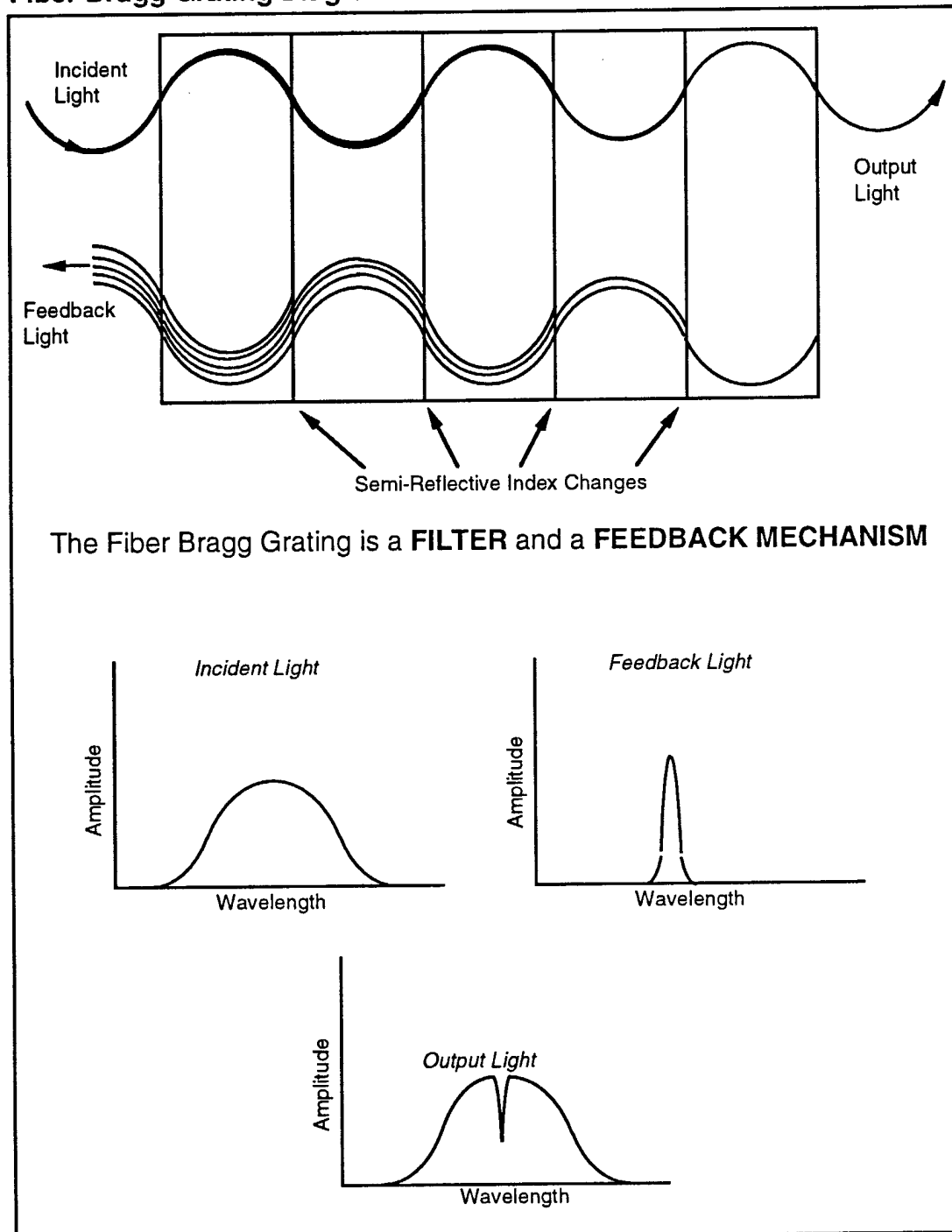
Wavelength

The fiber Bragg grating provides both feedback and filtering. The light which it filters out of its input is fed back to the diode material. The missing wavelengths can be seen as a dark line in the output.
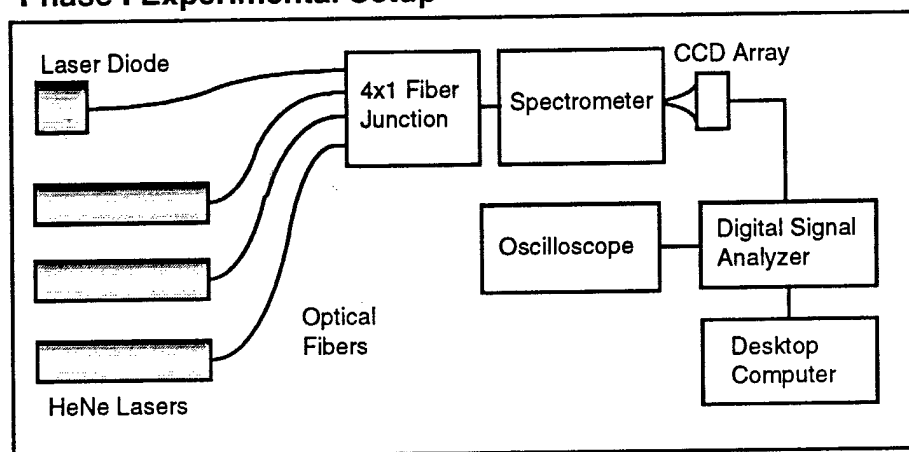
Figure 4

Compression

Incident Light

Output Light

Feedback Light

The Fiber Grating is **FLEXIBLE** and it can be **TUNED**.

Extension

Incident Light

Output Light

Feedback Light

Unstrained
The wavelength fed back by the grating depends upon the spacing of the grating surfaces.

Amplitude

Wavelength

Compression
The wavelength fed back by the grating decreases as the grating is compressed and the spacing in it decreases.

Amplitude

Wavelength

Extension
The wavelength fed back by the grating increases as the grating is extended and the spacing in it increases.

Amplitude

Wavelength

The Bragg grating can be tuned by changing its length and thus its internal spacing.   Figure 5

Phase I Experimental Setup

The experimental setup for Phase I was used to chacterize
the sensors used in this research and the laser diode used in
the tunable laser.

Figure 6

Spectrometer / CCD Array Diagram

Input Light   Spectrometer   Spectrometer Output

λ_1
λ_2

Amplitude
λ_1 λ_2
Wavelength

CCD Input   CCD Array   CCD Output

Amplitude
λ_1 λ_2
Wavelength

Amplitude
λ_1 λ_2
Wavelength
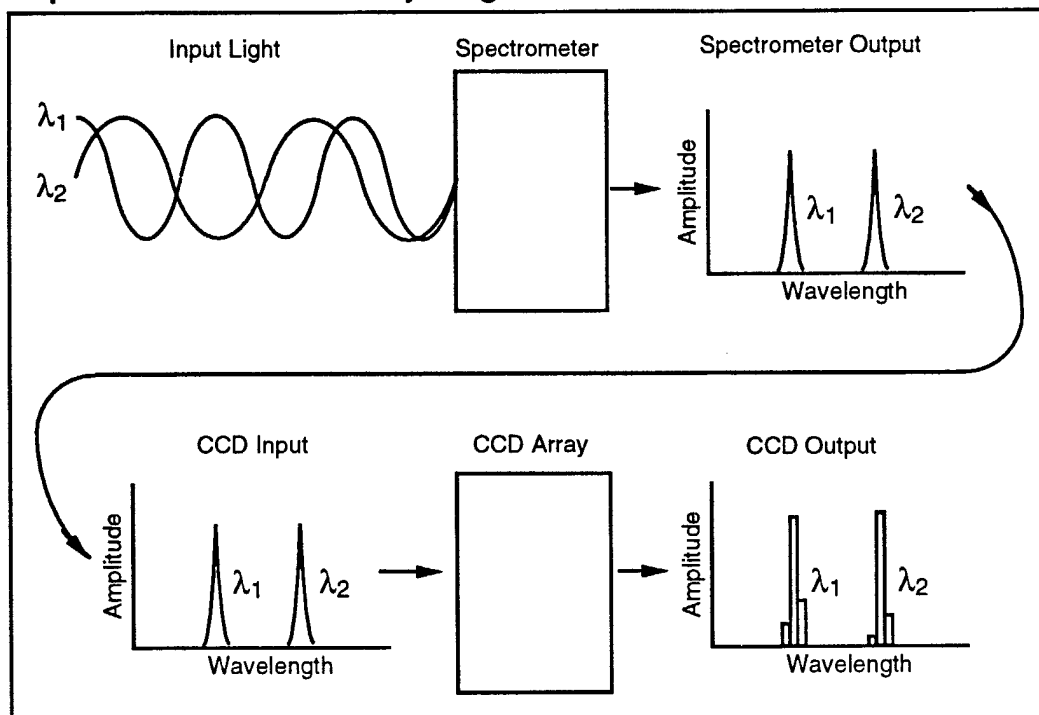
The spectrometer spreads incoming light into the component wavelengths.
It creates a spectrum of its input with wavelength on the x-axis and amplitude
on the y-axis. This image is then digitized by a charge-coupled device array.

Figure 7

Czerny-Turner Spectrometer
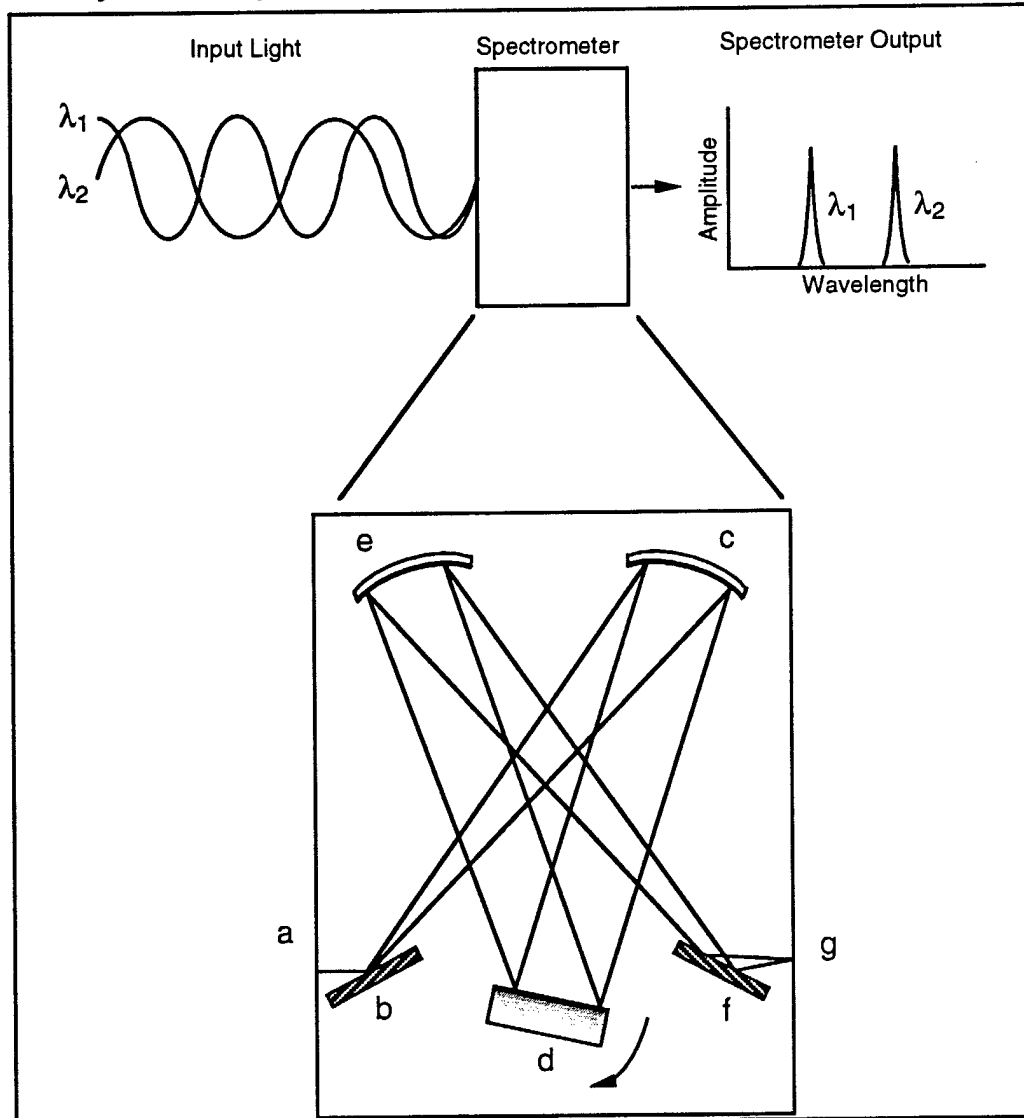
The Czerny-Turner configured spectrometer divides the input light into component wavelengths and displays their relative intensities. Diagram: a. Input Aperture. b. Input Minor Mirror. c. Input Collimating Mirror. d. Blazed Dispersion Grating. e. Output Converging Mirror. f. Output Minor Mirror. g. Output Aperture.

Figure 8

Dispersion Diagram

Spectrum One

Amplitude

$\Delta\lambda_1$

λ_a λ_b

Wavelength

The **dispersion** of a spectrometer is the **scale** of the wavelength axis of its output.

Spectrum Two

Amplitude

$\Delta\lambda_2$

λ_a λ_b

Wavelength

$\Delta\lambda_1 < \Delta\lambda_2$

Therefore, we say that the **dispersion** of spectrum one is **less than** the **dispersion** of spectrum two.
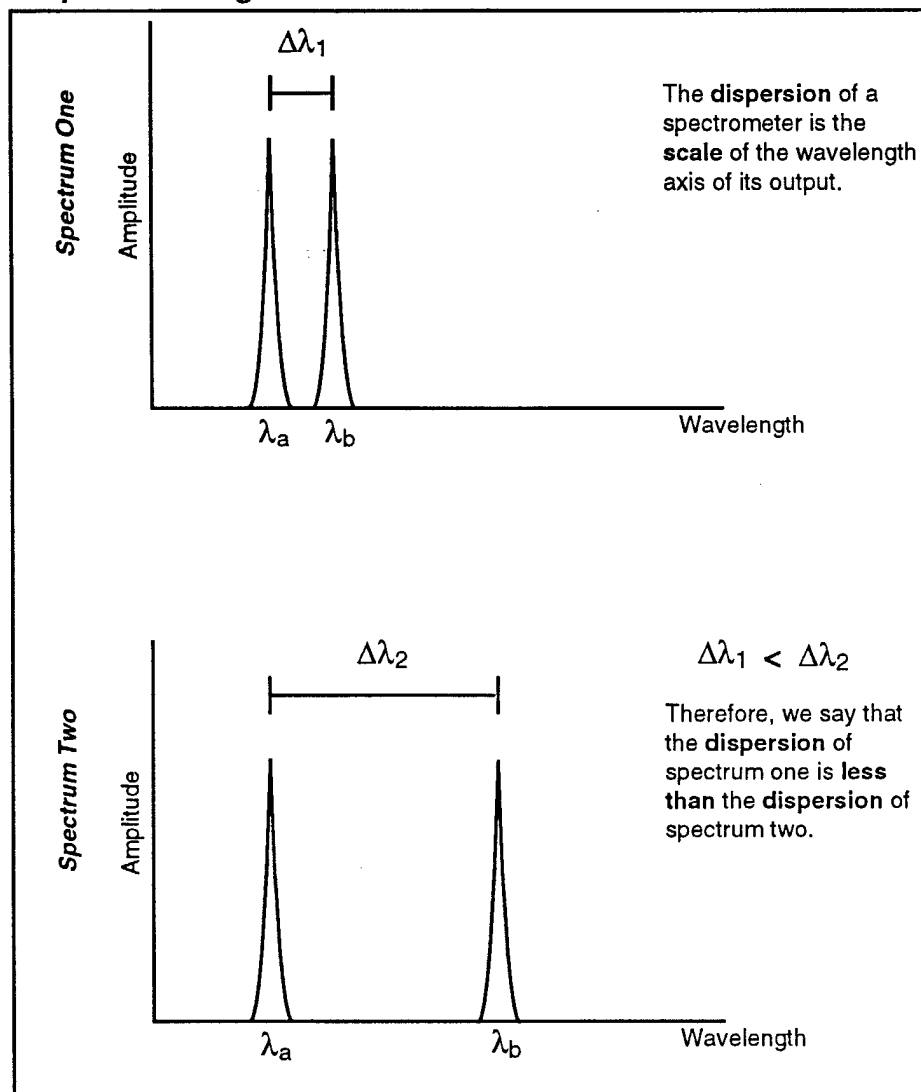
Dispersion is the scale of the wavelength axis of the spectrometer output.

Figure 9

$$n\lambda = a \cdot \sin\theta$$
$$n = order;$$

For constructive interference upon reflection, the path length difference between the reflected waves must be an integral multiple of the wavelength. Here, that path length difference is a•sinθ.
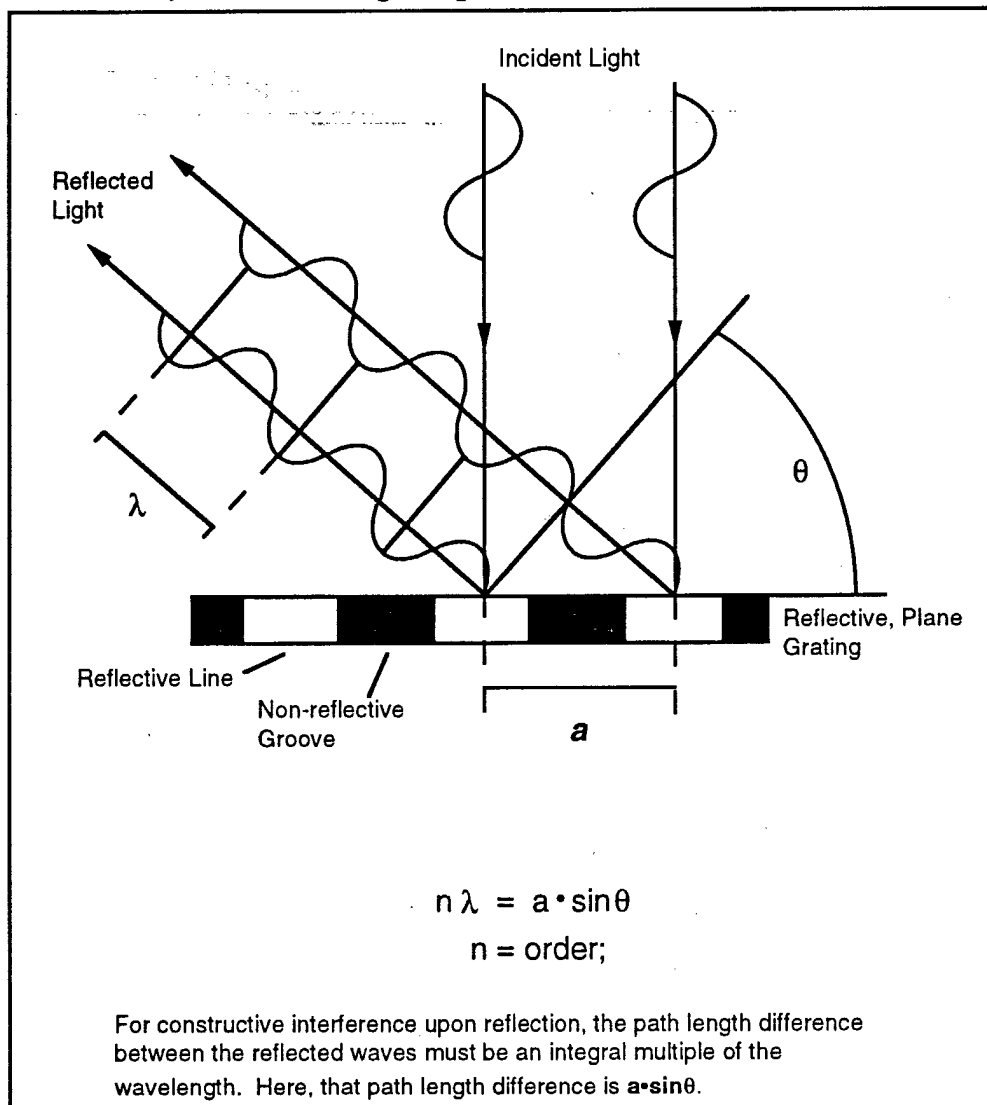
A reflective plane grating gives the spectrometer its ability to spread incoming light into component wavlengths. When the path difference between similar reflected rays is an integral multiple of their wavelength, those waves interfere constructively and a bright line appears at the spectrometer output. Different wavelengths will interfere constructively at different angles from the grating normal.

Figure 10

Resolution Diagram

Spectrum One

Amplitude

$\Delta\lambda_1$

h

$h/2$

λ_a

Wavelength

The **resolution** of a spectrometer refers to the **spreading** of an arbitrarily narrow input.

The *width* of an image is measured at its *half-maximum*.

Spectrum Two

Amplitude

$\Delta\lambda_2$

h

$h/2$

λ_a

Wavelength

$\Delta\lambda_1 < \Delta\lambda_2$

Therefore, we say that the **resolution** of spectrum one is **greater than** the **resolution** of spectrum two.
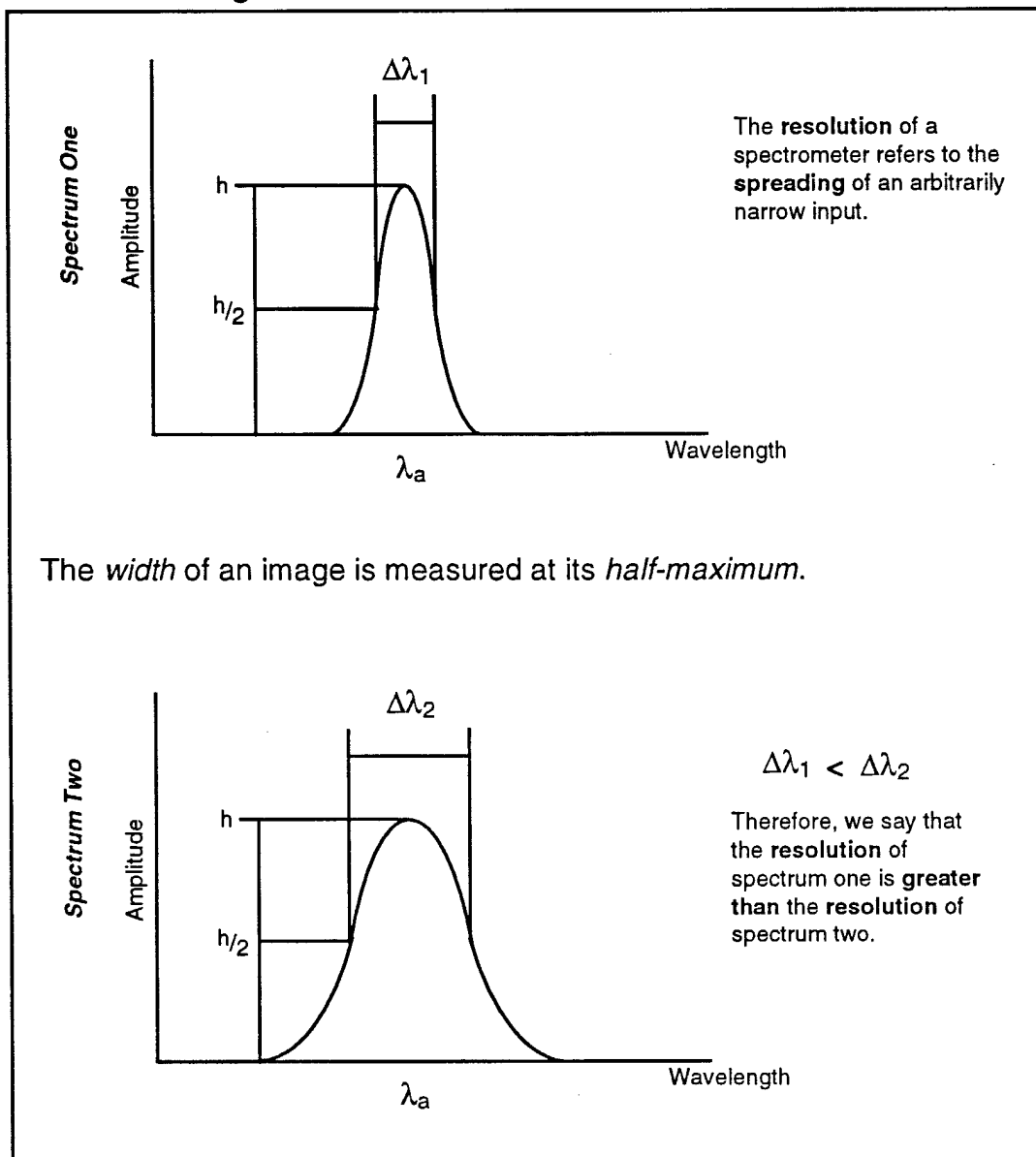
Resolution is the sharpness of the spectrometer output. Good resolution will not broaden an image too much.

Figure 11

Figure 12--Plot of Image Width
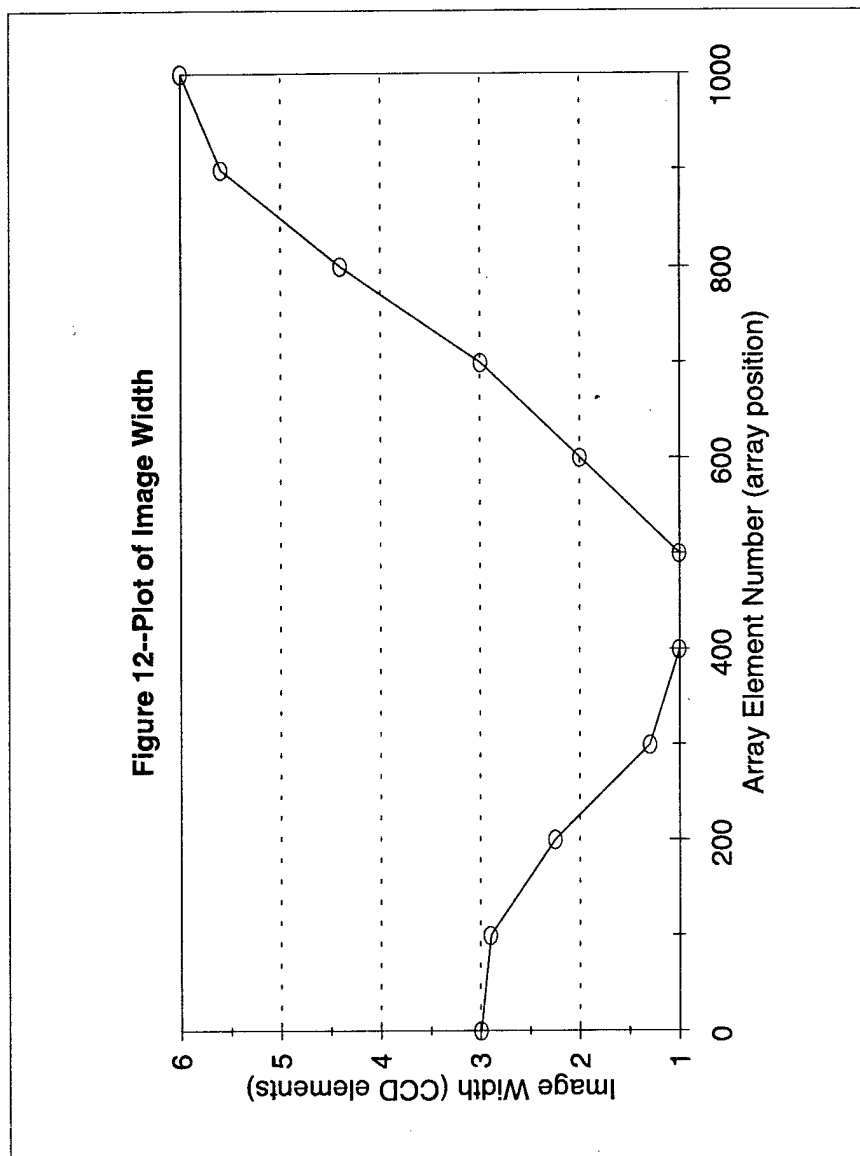
The Plot of Image Widths shows that there is a region between CCD element 400 and 500 where the resolution is as good as we predicted. The greater image widths on the fringes is due to instrument focus.

Czerny-Turner Output Configuration
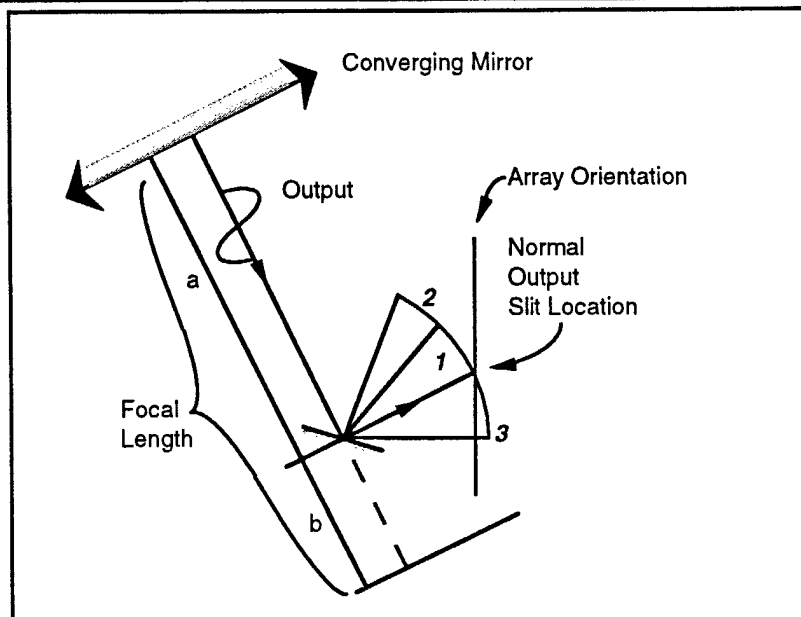
The Czerny-Turner spectrometer uses a converging mirror to focus the reflections from the grating toward the output slit. It then uses another, smaller mirror to direct this image to the output slit. When a long array is subsitituded for a narrow slit, some focus problems occur with this configuration.

Optimum focus, location f, occurs when the image is directed at the normal output slit location. To the left and right of that position, the focus occurs before or behind the CCD array and the resulting data is blurry.
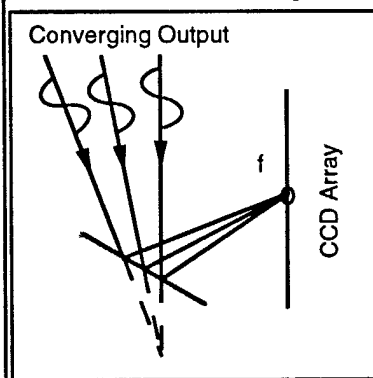
1: Focus at the Array   **2: Focus Before the Array**   **3: Focus Behind the Array**
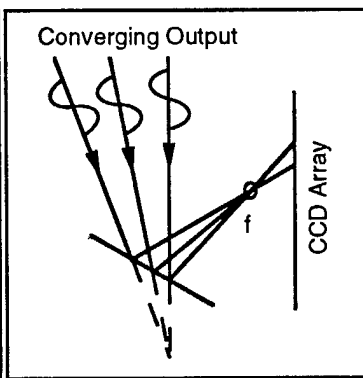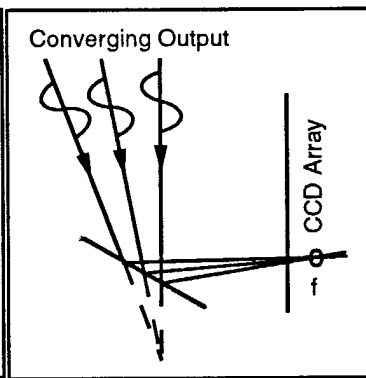
Figure 13

## Figure 14--Laser Diode Mode Structure
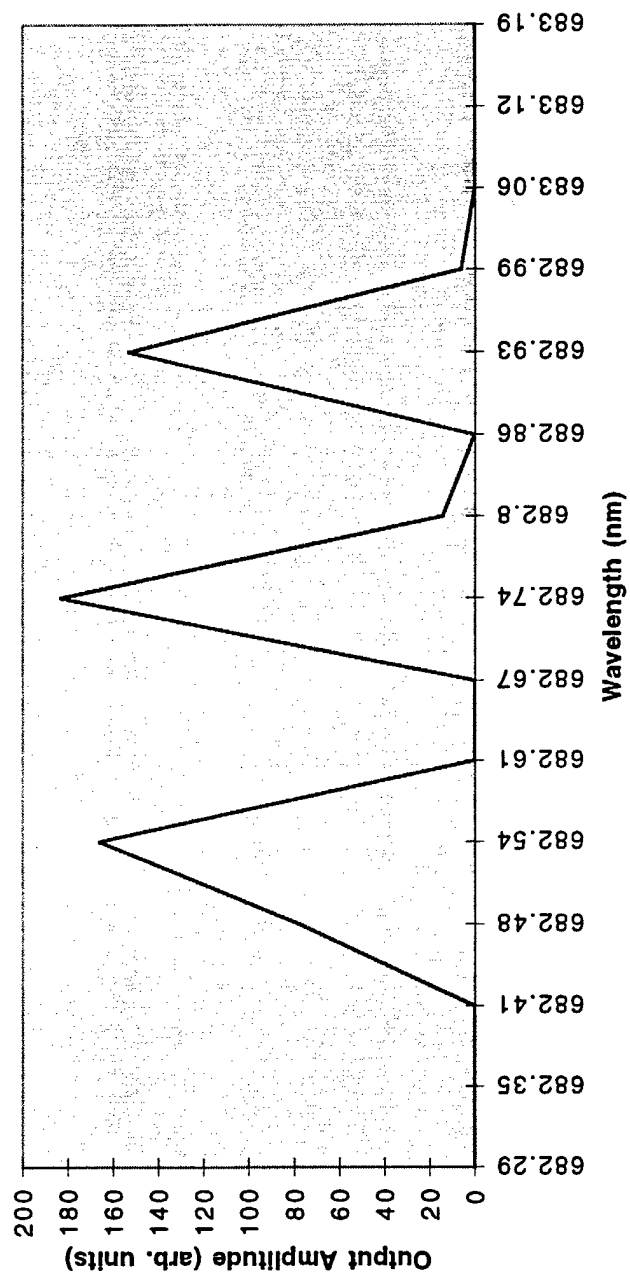
The resolution of the spectrometer and CCD array combined was fine enough to view the mode structure of the laser diode. Modes are separated by 2.5 Å.

Figure 15--Laser Diode Spectrum at 25 mA
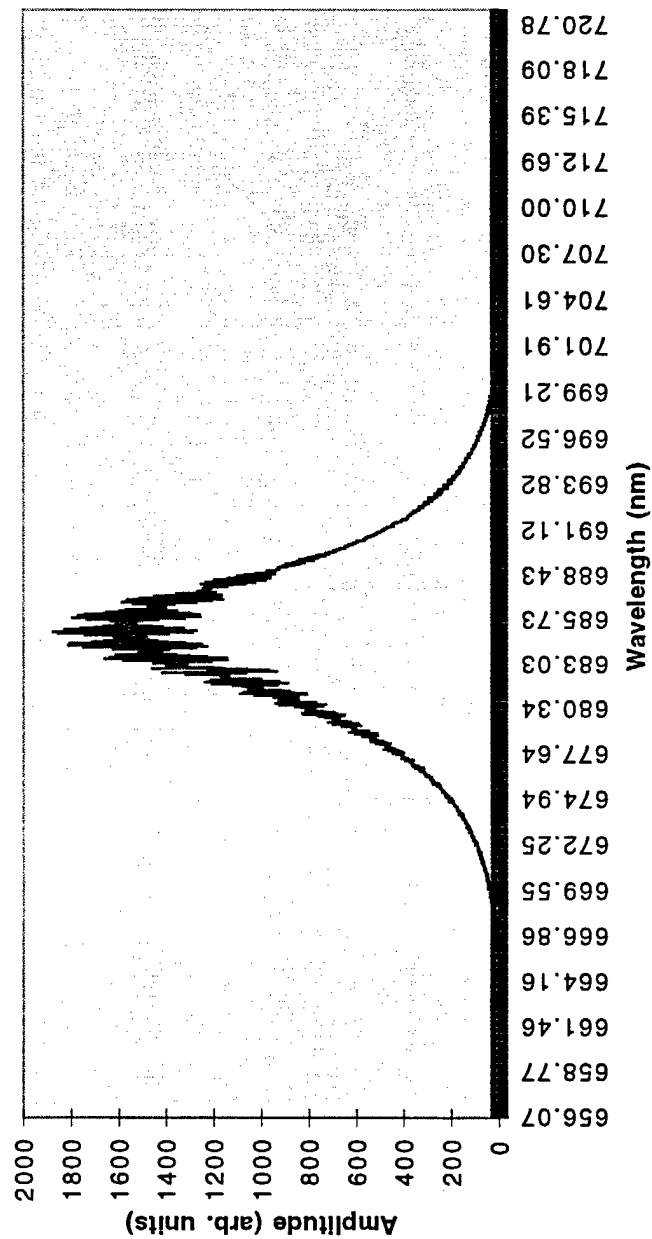
The laser diode emits a broad band of wavelengths at low power levels. Approximate bandwidth here is ten nanometers.

**Figure 16--Laser Diode Spectrum at 33 mA**
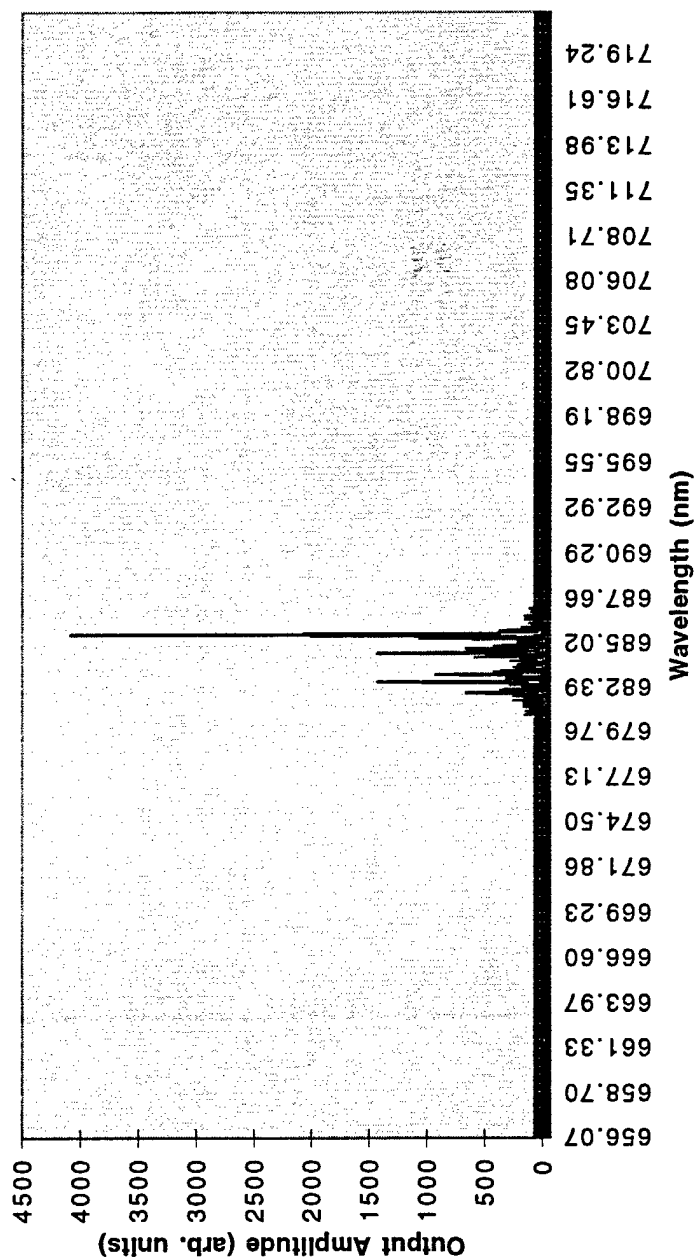
As the drive current increases, the laser diode begins to select one of its modes. The gain curve narrows toward the center of the broad band spectrum. One mode begins to predominate at this location.

Figure 17–Laser Diode Spectrum at 47 mA
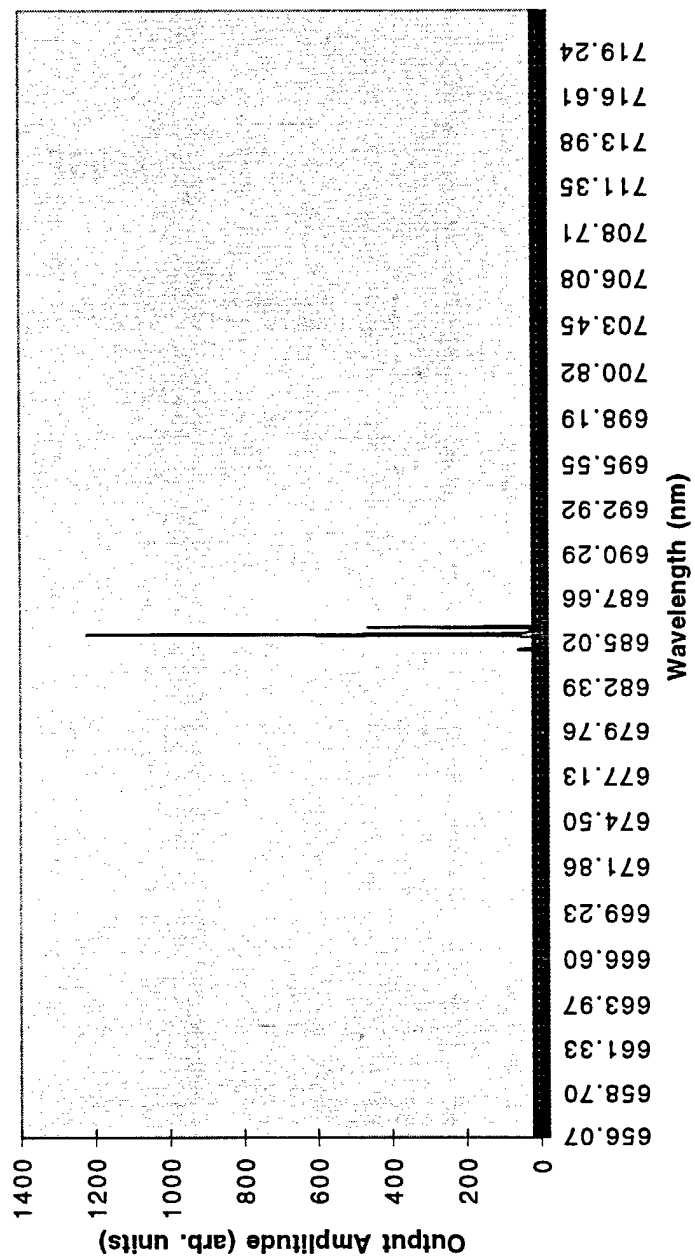
The laser diode is operating in its single mode regime. Here the gain curve is not perfectly centered on the predominant mode, so a neighboring mode shows some amplitude.

Figure 18--Laser Diode Mode Selection
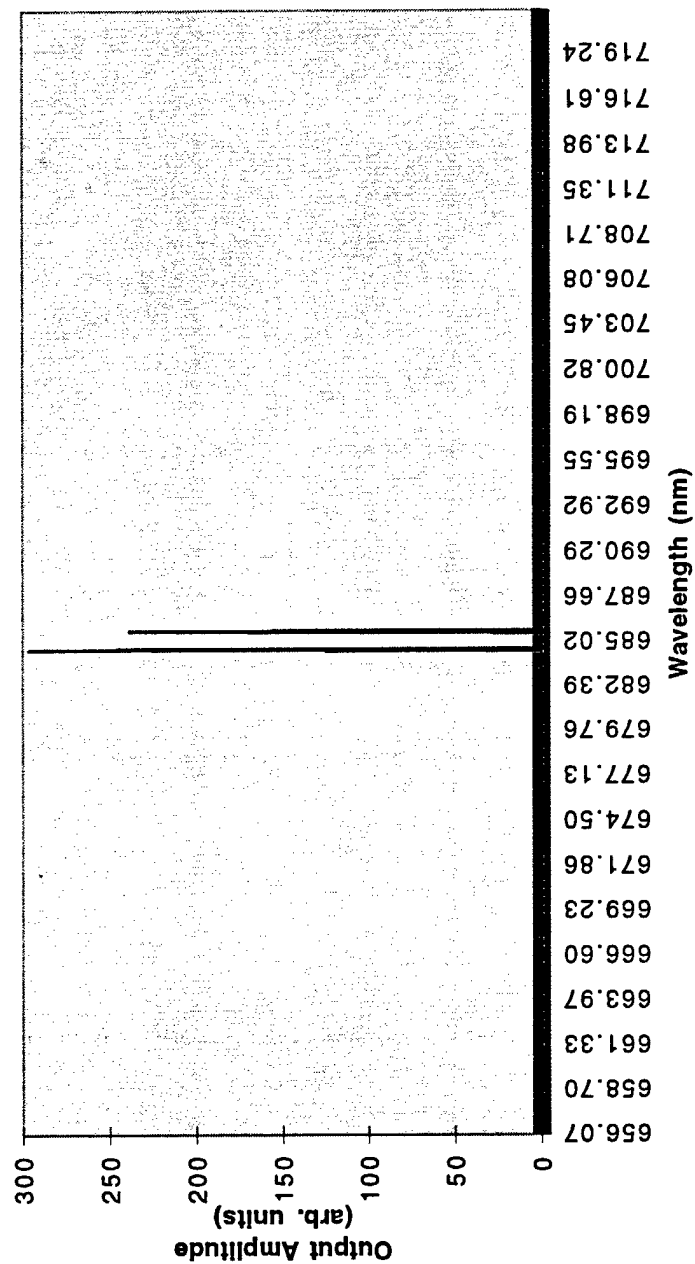
As the laser diode redshifts, higher modes fall under the gain curve and lower modes fall out of it. Here the gain curve is roughly centered over two neighboring modes. The mode to the right will continue to be selected as the drive current is increased while the mode to the left will be attenuated.
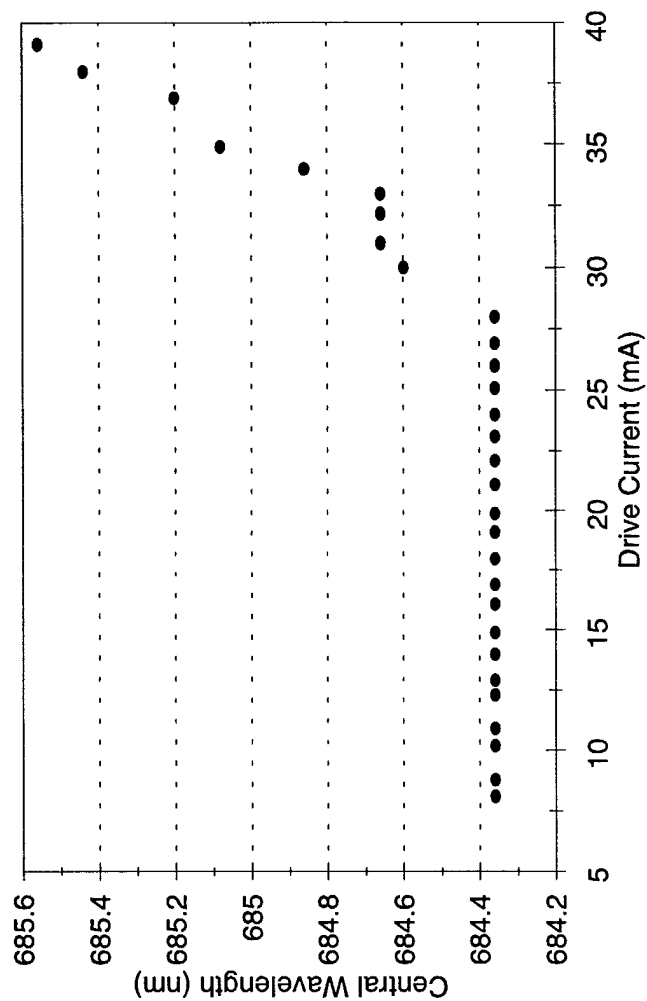
Figure 19--Output Power vs. DC
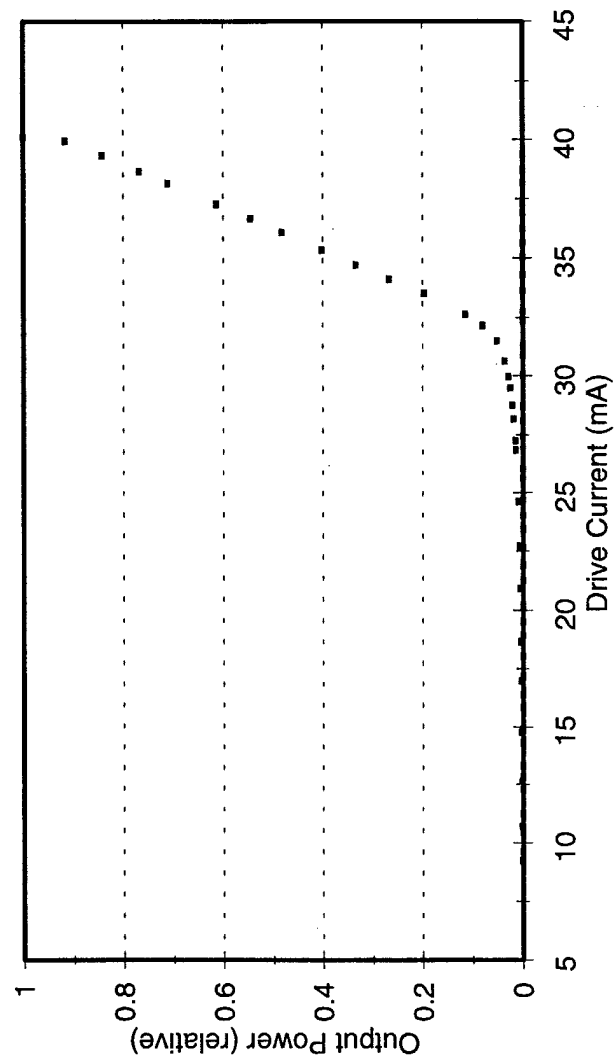
The laser diode exhibits a shift to its laser regime in the vicinity of thirty milliamps.
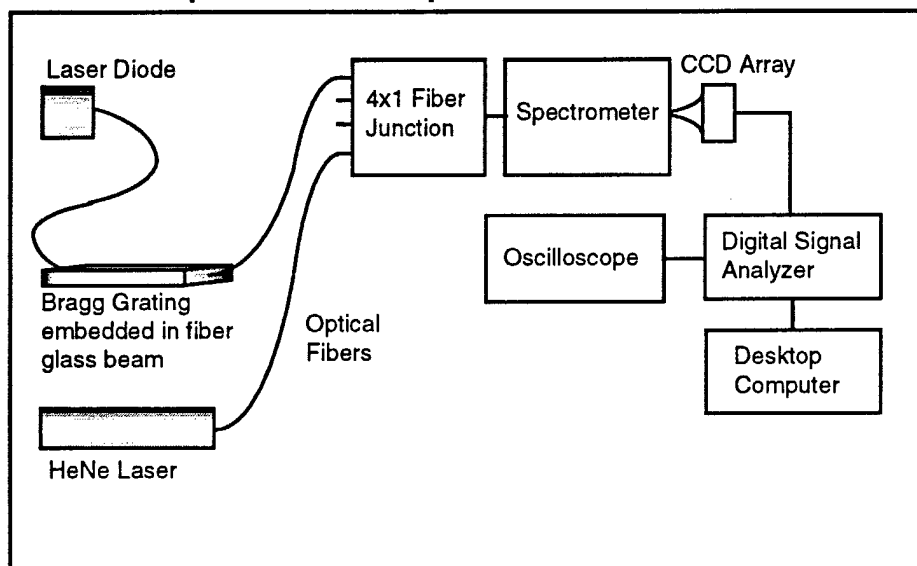
Figure 20--Diode Bandwidth vs. DC
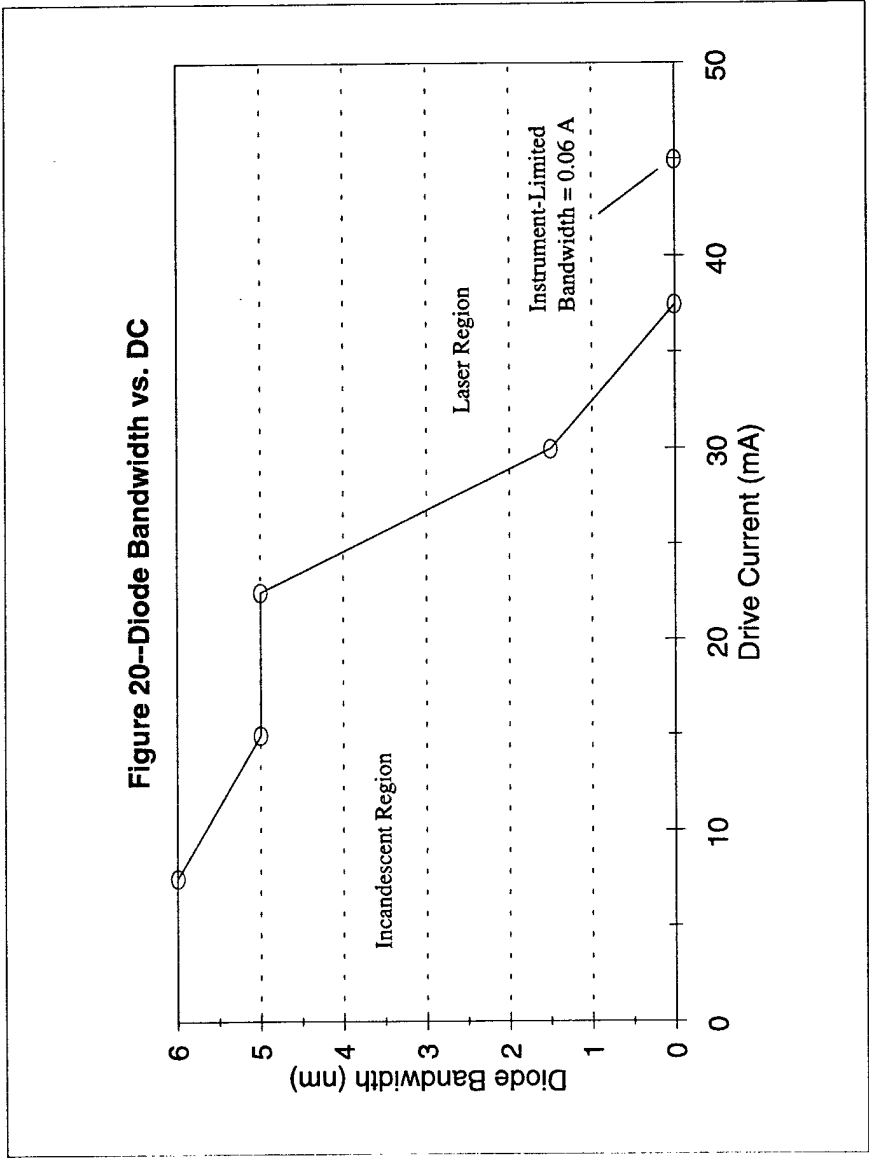
The laser regime of the laser diode is characterized by a sudden drop in the width of the gain curve and thus the output bandwidth.

Figure 21--Central Wavlength vs. DC

The laser diode begins to redshift as the drive current is increased in the laser state. This shift is due to electronic structure changes in the gain medium due to the higher drive current.
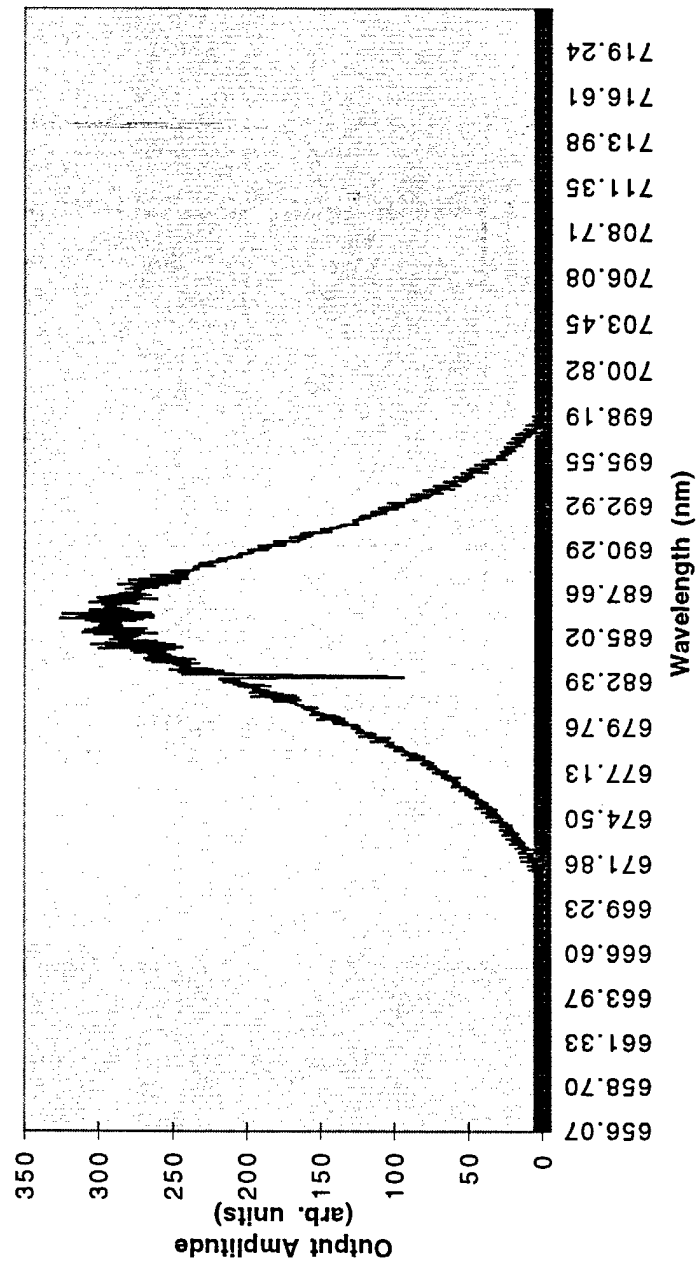
Phase II Experimental Setup

The grating and its tuning apparatus have been placed in the experimental setup in Phase II.

Figure 22

Figure 23--Laser Spectrum at 18.7 mA

At low power, the output of the tunable laser shows the filtering effect of the fiber grating. The dip in the spectrum at 682.6 nanometers is caused by the grating filtering this wavelength out and feeding it back to the laser diode.

Figure 24--Tunable Laser Output Spectrum at 32.3 mA
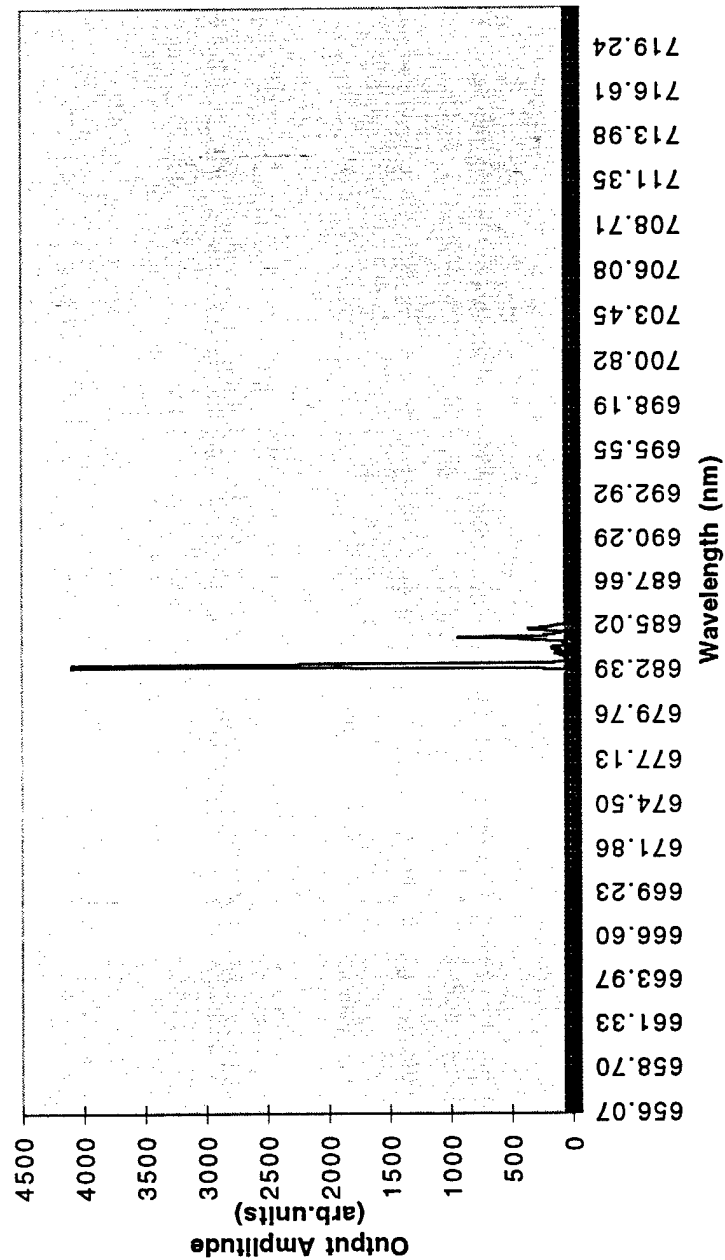
In the vicinity of thirty milliamperes, the tunable laser begins to lase at the Bragg wavelength of the grating. Other modes are suppressed by the strong presence of the Bragg feedback in the laser diode gain medium.

Figure 25--Tunable Laser Output Spectrum at 36 mA
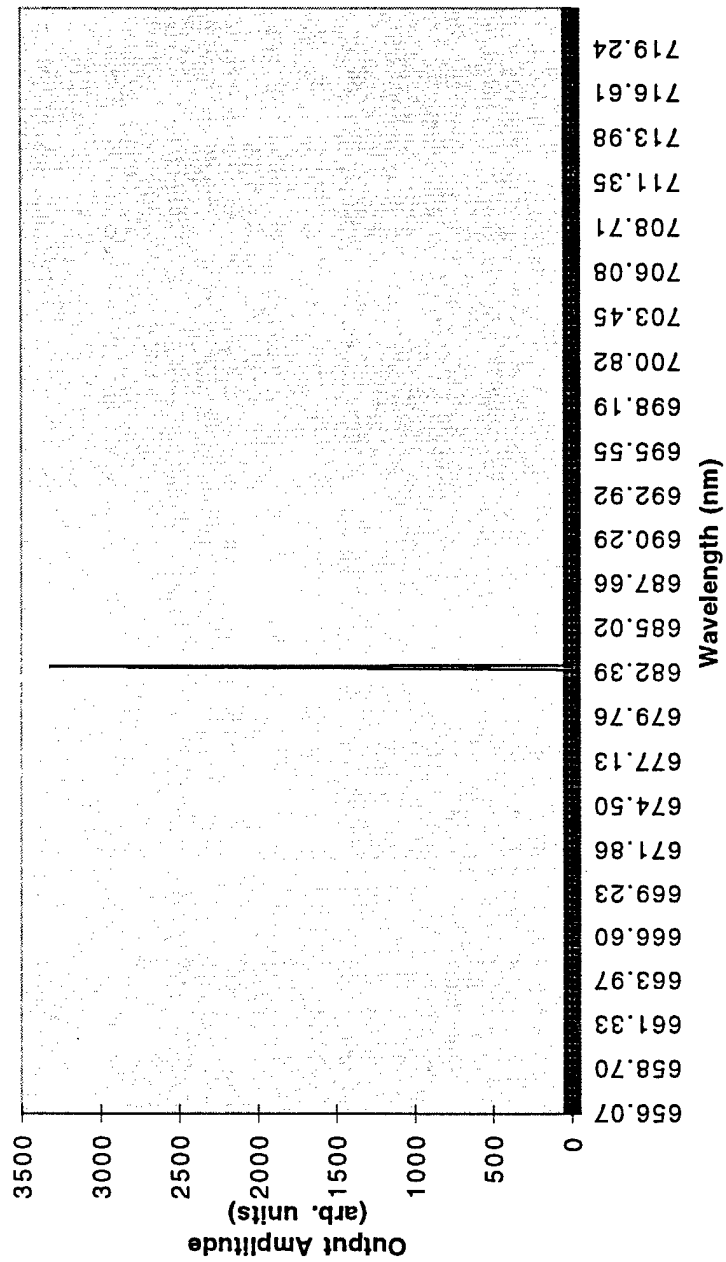
The tunable laser is operating in a single-mode state, with the Bragg wavelength selected from the laser diode's broad comb of modes.

Figure 26--Power vs. Drive Current
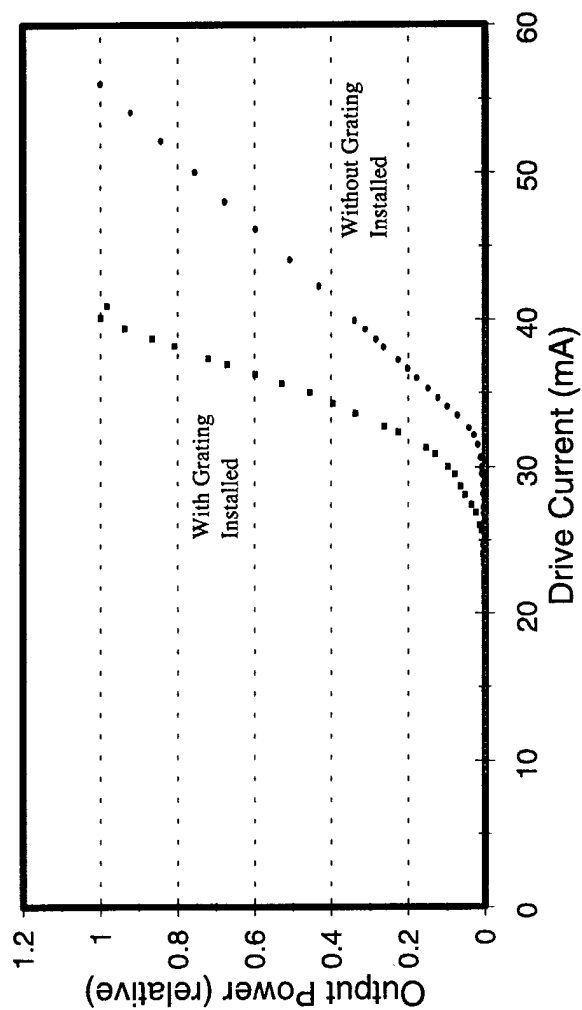
A comparison of the output powers of the phase I and phase II systems shows that the addition of the fiber grating caused the laser diode to roll off into its laser state at a lower drive current. The grating also increased the slope of the power curve in the laser state.

Fiber Grating Strain Device
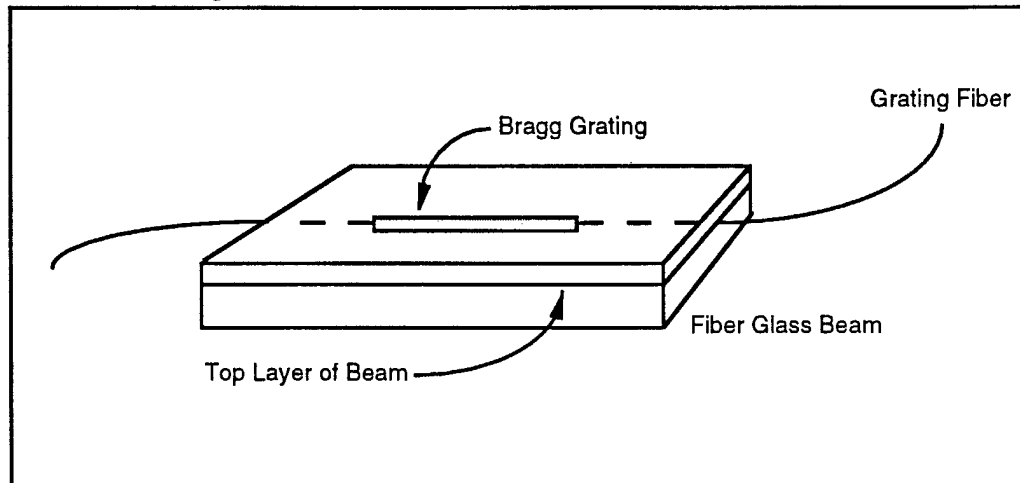
The fiber Bragg grating is prepared for straining by embedding it in the top layer of a composite fiber glass beam.

Figure 27

Fiber Grating Straining Method Diagram

The Top Surface is Extended.

Grating
Fiber

Radius of Curvature

R

τ

Thickness of Beam

The Bottom Surface is Compressed.

$$\sigma = \tau/2R$$

where: $\quad \sigma \equiv \dfrac{\Delta L}{L_o}$

such that: $\quad \sigma =$ Strain

$L_o =$ Initial Length

$\Delta L =$ Change in Length
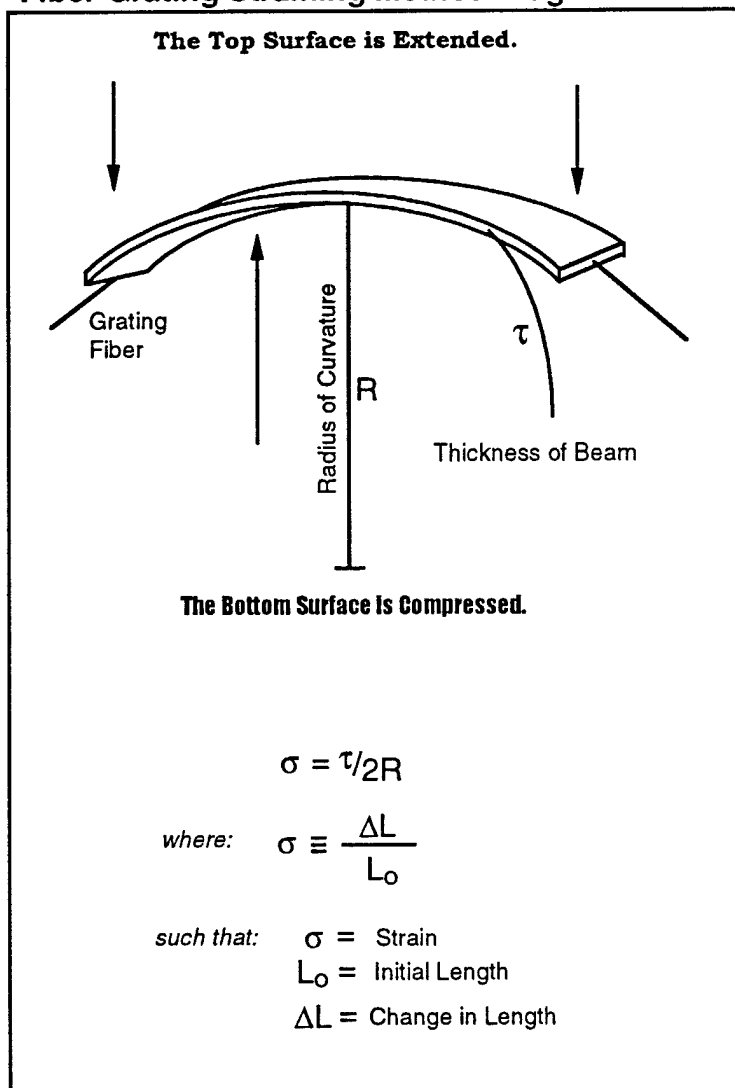
The fiber Bragg grating is strained by deflecting
the fiber glass beam which contains the grating.

Figure 28

Figure 29--Laser Tunability

The tunable laser was tunable over a range of about five nanometers.
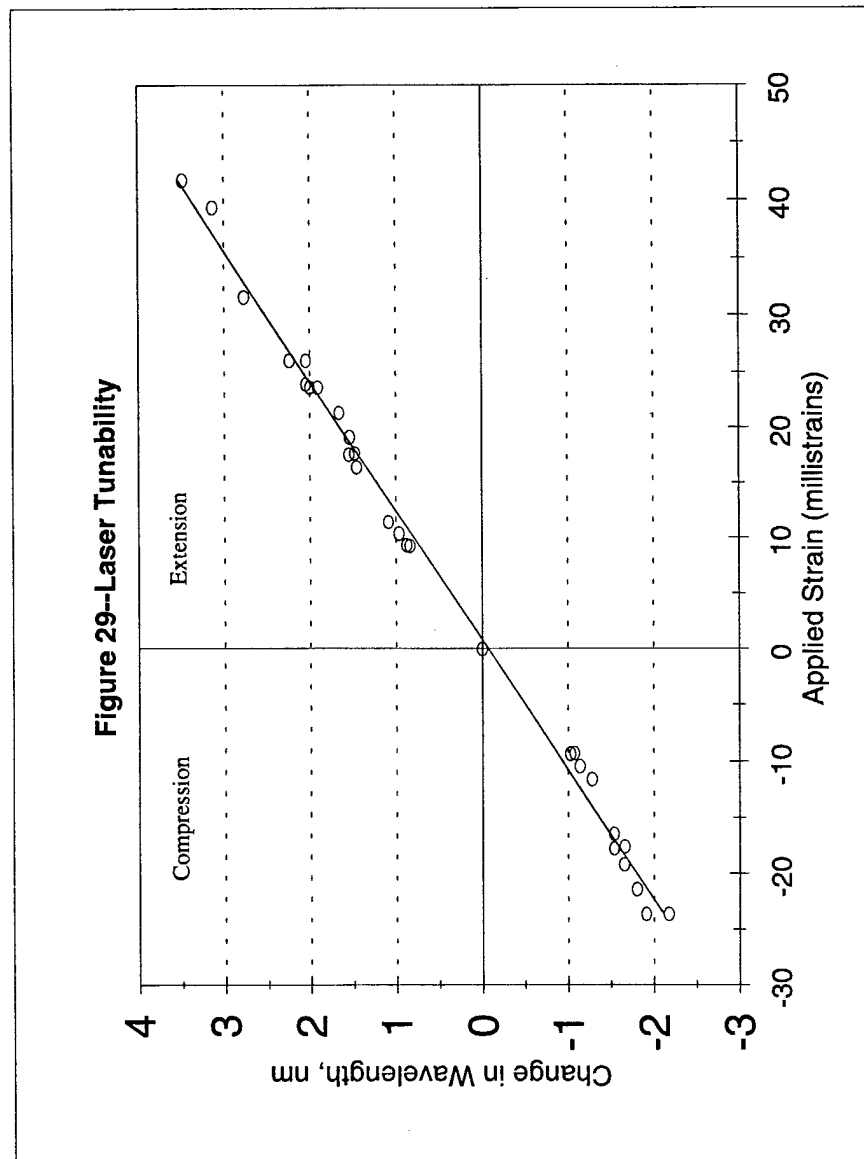
Figure 30--Some Tuned States of the Laser
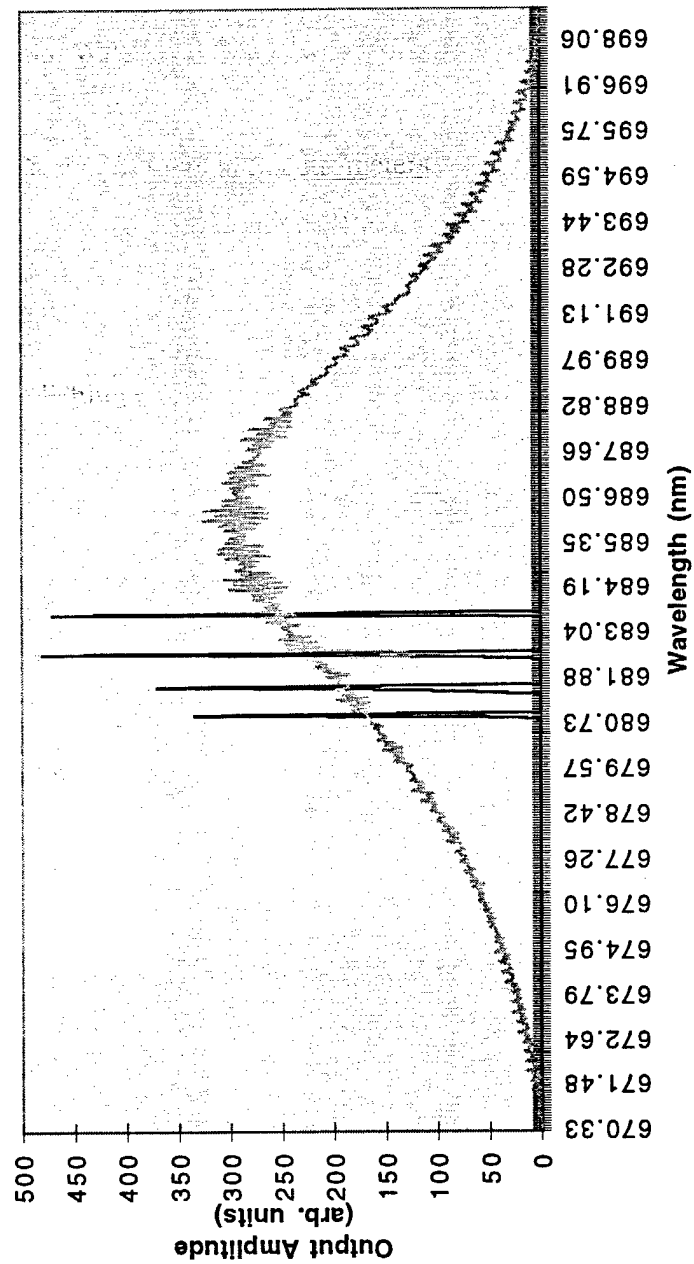
Some of the tuned states of the tunable laser are shown here with the laser diode's broadband spectrum superimposed.

46

Figure 31--Some Adjacent Available Output Modes of the Tunable Laser

Three adjacent output modes of the tunable laser are shown here. From the center mode, the mode to the left is the next available mode if we compress the grating. The mode to the right is the next available mode if we extend the grating.

Endnotes

1. Nehrich, Richard B., <u>Atomic Light: Lasers-What They Are and How They Work</u>, Sterling Publishing Co., Inc., New York, NY, 1967, pp. 56-87.

2. *Ibid.*, pp. 11-20.

3. *Ibid.*

4. Wagreich, R. B, and J.S. Sirkis, "Distinguishing Fiber Bragg Grating Strain Effects", in <u>Twelfth International Conference on Optical Fiber Sensors</u>, Vol. 16, OSA Technical Digest Series (Optical Society of America, Washington DC, 1997), pp. 20-23.

5. *Ibid.*

6. James, J. F., <u>The Design of Optical Spectrometers</u>, Chapman and Hall LTD., London, 1969, pp. 43-61.

7. *Ibid.*, pp. 9-10.

8. Coldren, L.A., and S. W. Corzine, <u>Diode Lasers and Photonic Integrated Circuits</u>, John Wiley and Sons, New York, 1995, p. 138.

9. *Ibid.*, p. 66.

10. *Ibid.*, p. 60.

Bibliography

Coldren, L.A., and S. W. Corzine, <u>Diode Lasers and Photonic Integrated Circuits</u>, John Wiley and Sons, New York, 1995.

James, J. F., <u>The Design of Optical Spectrometers</u>, Chapman and Hall LTD., London, 1969.

Nehrich, Richard B., <u>Atomic Light: Lasers-What They Are and How They Work</u>, Sterling Publishing Co., Inc., New York, NY, 1967.

Wagreich, R.B., and J.S. Sirkis, "Distinguishing Fiber Bragg Grating Strain Effects", in <u>Twelfth International Conference on Optical Fiber Sensors</u>, Vol. 16, OSA Technical Digest Series (Optical Society of America, Washington DC, 1997), pp. 20-23.

Appendix A: Dispersion

Light input to the spectrometer disperses upon reflection from a plane grating. When these diffraction patterns, sometimes called *wavelets*, interfere constructively, they create bright lines in the spectrometer output. In order to interfere constructively, these wavelets must fill the conditions shown below.

Reflective, Plane Grating Diagram
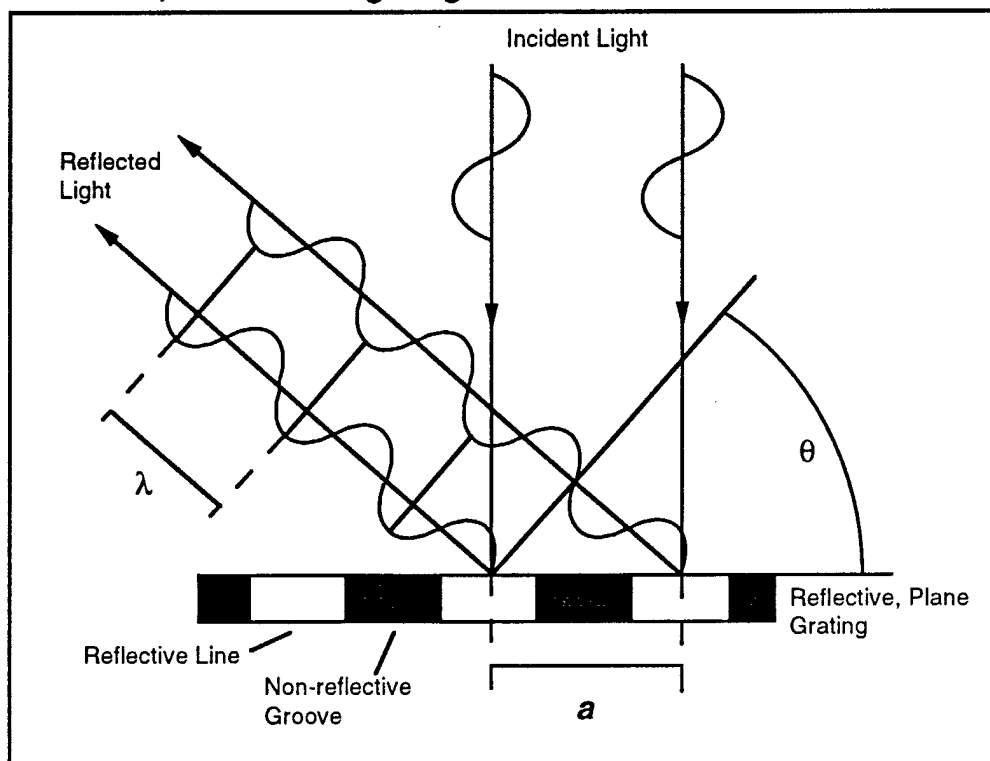
The reflective plane grating in the spectrometer spreads incoming light into component wavelengths according to the angular relationship shown.

Figure A1

$$n\lambda = a \cdot \sin\theta \qquad \text{(A1)}$$

where: n = an integer;

λ = wavelength;

a = the groove spacing
of the reflective grating,
here .00000167 m;
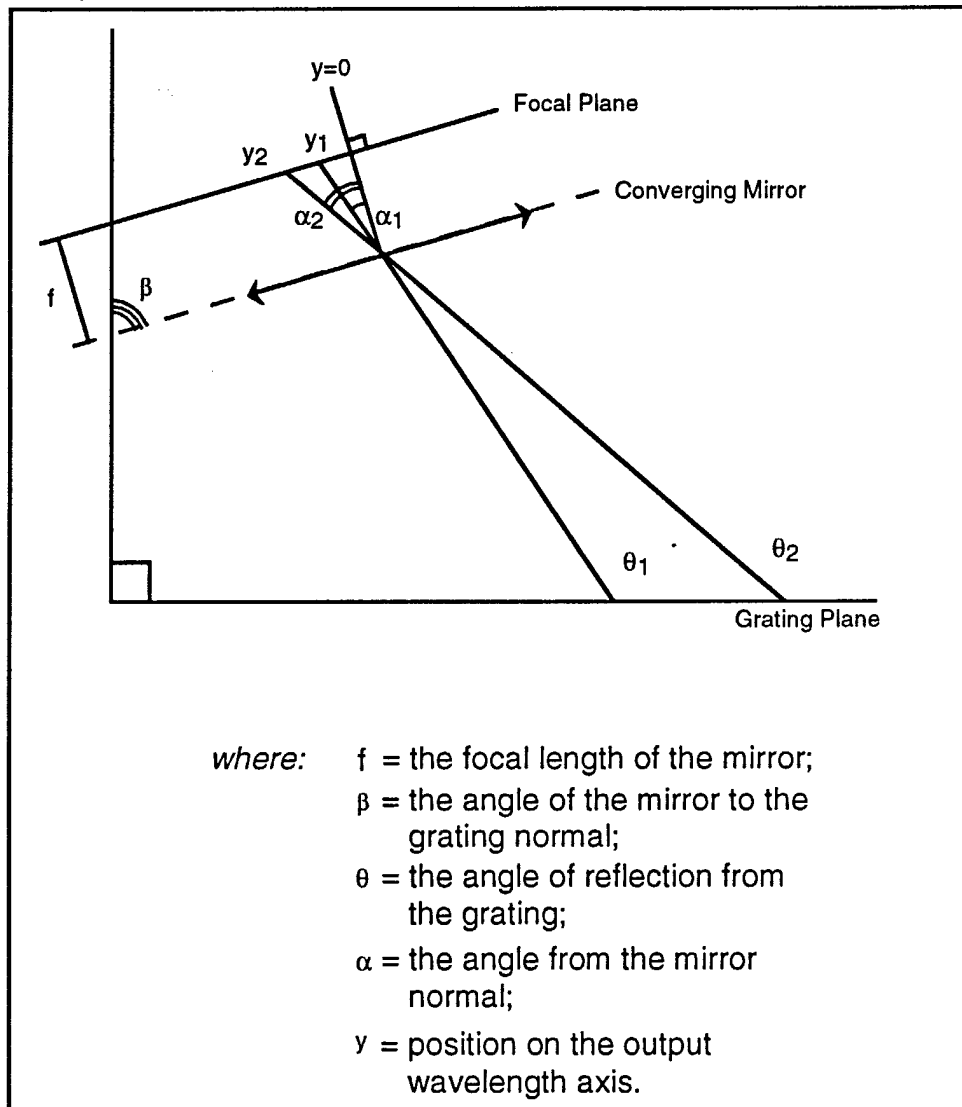
θ = the angle of reflection.

From equation (A1), it can be seen that each wavelength input to the spectrometer will interfere constructively at a different angle from the grating normal. This means that the grating has spatially separated the wavelengths of the input. An expression for dispersion is determined by the relationship between wavelength and reflection angle. The change in angle for a given change in wavelength can be calculated from equation (A1).

$$n \lambda = a \cdot \sin\theta$$

$$\frac{\delta\lambda}{\delta\theta} = \frac{a}{n}\cos\theta \qquad \text{(A2)}$$

Equation (A2) is an expression for the relationship between the change in wavelength and the change in reflection angle. Given the construction of the spectrometer, the reflection angle for any orientation of the grating could be measured. In the middle of the third order image of the visible spectrum, for example, the reflection angle was approximately forty five degrees. Since the theoretical values of the dispersion were derived only to provide a relative check of the measured values of dispersion, an approximate value for the angle of reflection was sufficient. The geometry shown in Figure (A2) was used to determine the relationship between reflection angle and position on the output wavelength axis.

Angular Conversion to Plane Output Diagram

where: f = the focal length of the mirror;

β = the angle of the mirror to the grating normal;

θ = the angle of reflection from the grating;

α = the angle from the mirror normal;

y = position on the output wavelength axis.

The spectrometer uses a converging mirror to transform the angular spreading of wavelengths into a linear spreading of wavelengths.

Figure A2

Figure (A2) shows the relationship between the angle of reflection from the grating and the position of a bright line on the wavelength axis of the output. This relationship is described by the following equations:

$$\theta_n = \alpha_n + \beta_n - 90° \qquad (A3)$$

$$\delta\theta_n = \delta\alpha_n \qquad (A4)$$

$$y_n = f \cdot \tan \alpha_n \qquad \text{(A5)}$$

where, for small values of α_n:

$$y_n = f \cdot \alpha_n$$

$$\delta y_n = f \cdot \delta \alpha_n \qquad \text{(A6)}$$

Substituting equation (A4) into equation (A6):

$$\delta y_n = f \cdot \delta \theta_n$$

$$\frac{\delta \theta_n}{\delta y_n} = \frac{1}{f} \qquad \text{(A7)}$$

Finally, an expression for the dispersion of the spectrometer can be found by multiplying equations (A2) and (A7).

$$\frac{\delta \lambda}{\delta y} = \frac{a}{f \, n} \cos \theta \qquad \text{(A8)}$$

Equation (A8) describes the relationship between change in position on the output wavelength axis and change in actual wavelength--i.e., dispersion.

In order to measure the scale of the wavelength axis of the spectrometer, three Helium Neon Lasers, shown in the Lasers Table, were simultaneously input to the spectrometer.

The wavelengths of these lasers were known and the separation of their bright lines on the CCD array could be determined by measuring their time separation on the oscilloscope as it scanned the array.

Lasers Table

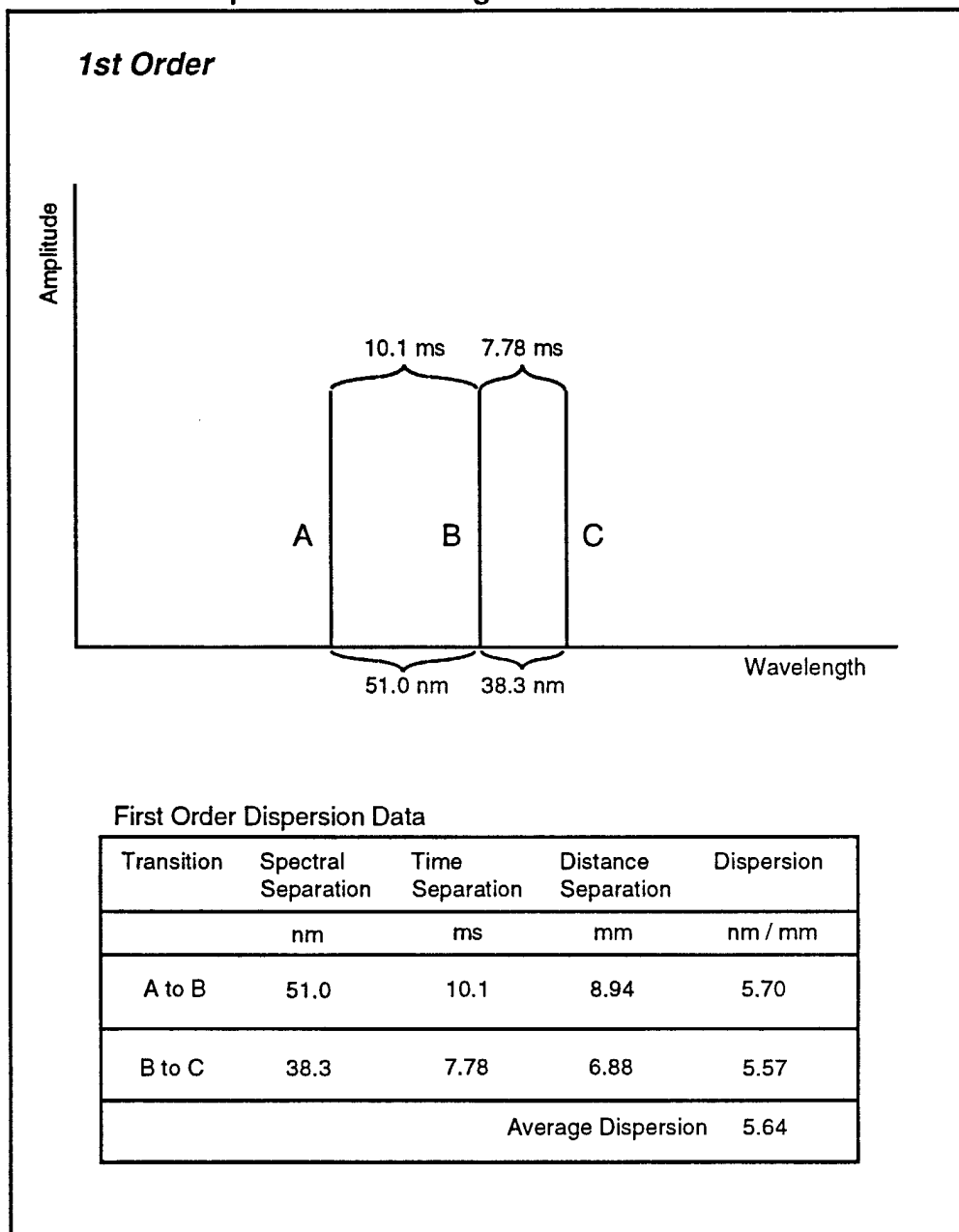| Laser	Color	Wavelength
A	Green	543.5 nm
B	Orange	594.5 nm
C	Red	632.8 nm

Table A1

The oscilloscope scanned the 1024 elements of the one-inch CCD array every 28 milliseconds. Equation (A9) shows the relationship between the time scale separation of two bright lines on the oscillscope and the actual distance between those bright lines on the CCD array (or in the spectrometer output).

1 mm on the array = 1.13 ms on the oscilloscope (A9)

The data collected for the measurement of dispersion in each order are shown below.

First Order Dispersion Data Diagram

1st Order

First Order Dispersion Data

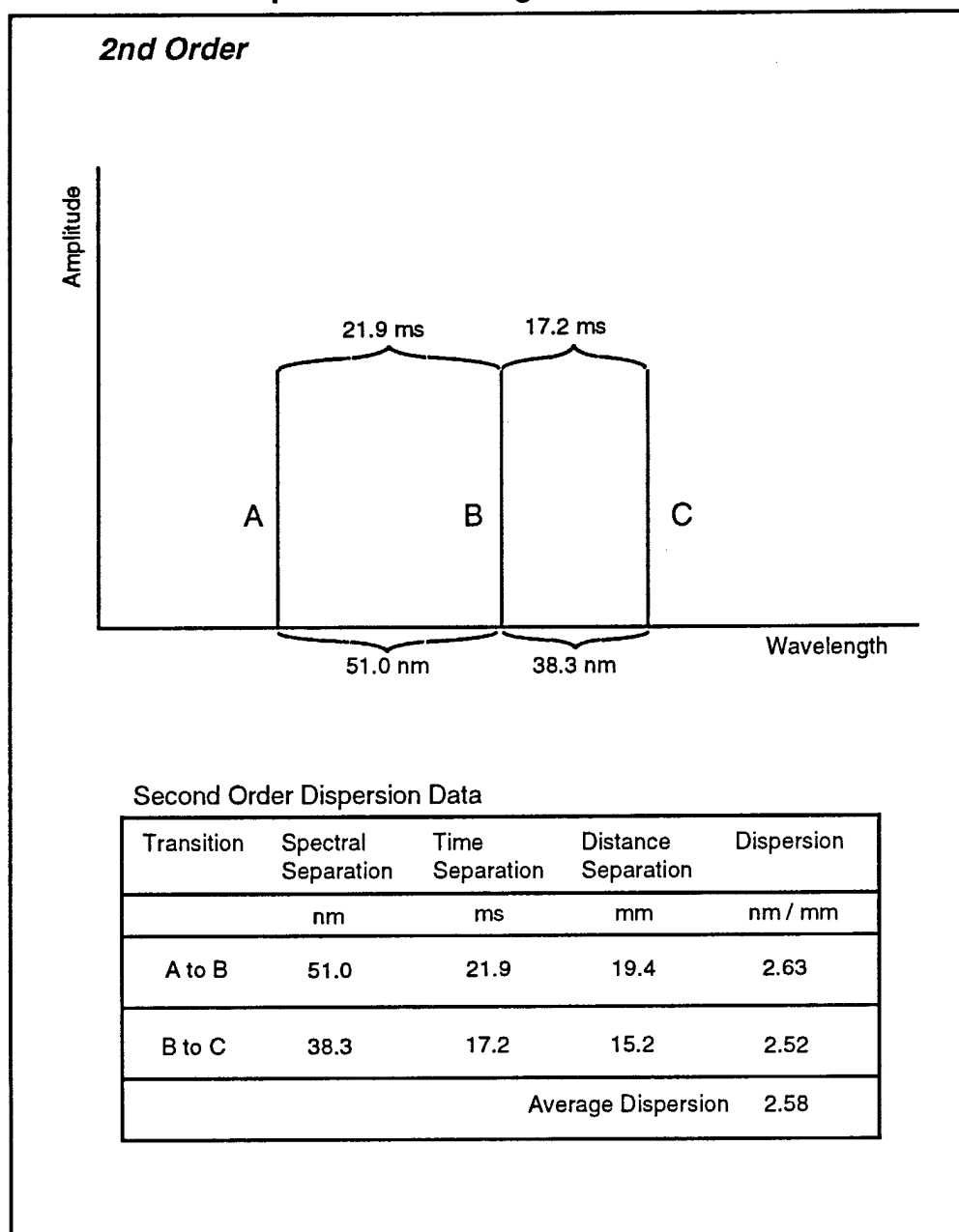| Transition	Spectral Separation	Time Separation	Distance Separation	Dispersion
	nm	ms	mm	nm / mm
A to B	51.0	10.1	8.94	5.70
B to C	38.3	7.78	6.88	5.57
			Average Dispersion	5.64

The dispersion measurement data for the first order image are shown.   Figure A3

Second Order Dispersion Data Diagram

2nd Order

Second Order Dispersion Data

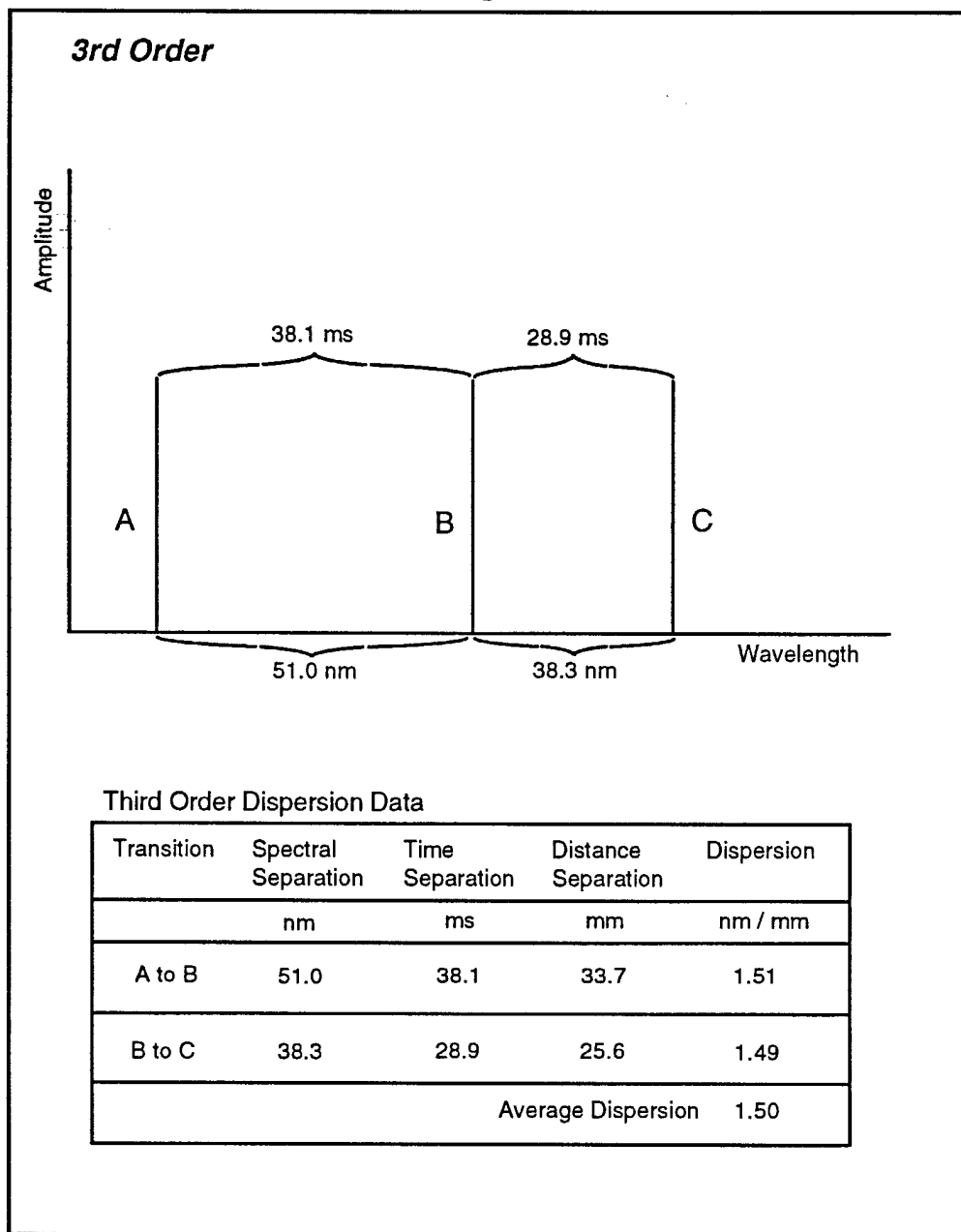| Transition	Spectral Separation	Time Separation	Distance Separation	Dispersion
	nm	ms	mm	nm / mm
A to B	51.0	21.9	19.4	2.63
B to C	38.3	17.2	15.2	2.52
			Average Dispersion	2.58

The dispersion measurement data for the second order image are shown.   Figure A4

Third Order Dispersion Data Diagram

Third Order Dispersion Data

Transition	Spectral Separation	Time Separation	Distance Separation	Dispersion
	nm	ms	mm	nm / mm
A to B	51.0	38.1	33.7	1.51
B to C	38.3	28.9	25.6	1.49
			Average Dispersion	1.50

The dispersion measurement data for the third order image are shown.　　Figure A5

Table A2 compares the values for dispersion predicted by Equation (A8) with those measured as shown above. The two sets of values compare favorably.
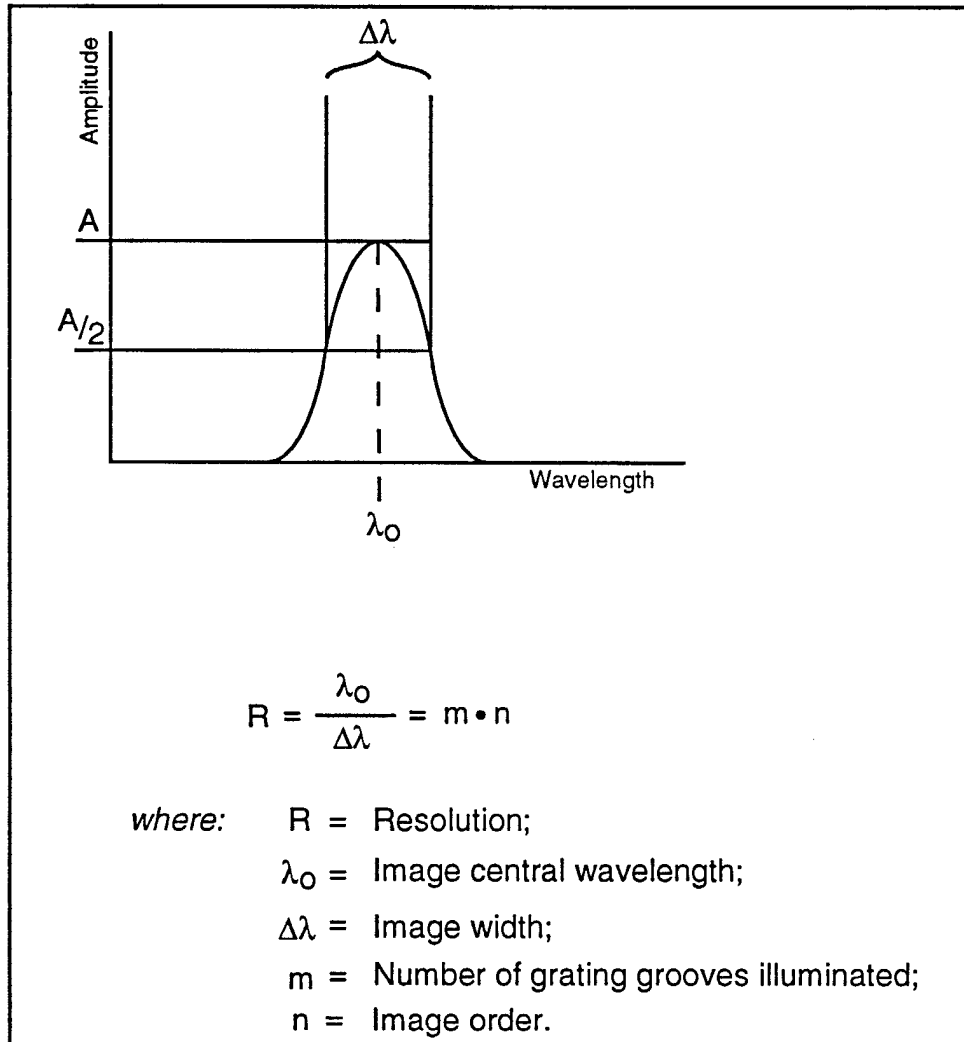
Predicted Dispersion vs. Measured Dispersion

Order	Predicted Value	Measured Value
1	5.8	5.64
2	2.6	2.58
3	1.5	1.50

Table A2

The **Resolution** of a spectrometer refers to the width of an output image corresponding to an input of arbitrarily narrow bandwidth. Resolution is quantified by dividing the central wavelength of an image in the output of the spectrometer to the width of that image at its half-maximum. This quantity is equal to the product of: the number of grooves being illuminated on the grating of the spectrometer by the input light; and the order of the image. Figure B1 shows these relationships.

Resolution Definition Diagram

$$R = \frac{\lambda_o}{\Delta\lambda} = m \cdot n$$

where: R = Resolution;

λ_o = Image central wavelength;

$\Delta\lambda$ = Image width;

m = Number of grating grooves illuminated;

n = Image order.

Resolution is a unitless quanitity which describes the broadening of an arbitrarily narrow image as a result of the optical mechanism of a spectrometer.

Figure B1

To measure the resolution of the spectrometer, light from a HeNe laser at 632.8 nm (red) was input to the spectrometer. The bandwidth of the laser was much narrower than the minimum instrument resolution. At the wavelength of the laser, in third order, and with approximately sixty millimeters of the 600 groove per millimeter grating illuminated, a predicted value for the image width was calculated:

$$R = \frac{\lambda_0}{\Delta\lambda} = m \cdot n$$

$$\Delta\lambda = \frac{\lambda_0}{m \cdot n}$$

for:

$\lambda_0 = 632.8$ nanometers;

$m = 36,000$ grooves;

$n = 3$rd order.

$$\Delta\lambda = 5.9 * 10^{-12}$$

$$\Delta\lambda = 0.06 \text{ Å}$$

$$R = 108,000$$

The predicted image width of the bright line of the HeNe laser was 0.06 Angstroms. The Resolution (unitless value) was 108,000.

Although the spectrometer output was 0.06Å wide, the CCD array could not accurately represent such narrowness, because its pixel size was much larger than this.

In third order, the wavelength axis of the spectrometer output is 38 nanometers long. The CCD array reads all of this with 1024 sensors spaced evenly over one inch. Each sensor therefore covers a region of the wavelength axis 0.371Å wide. This is the smallest unit of image width which can therefore be discriminated in the data. As a result, any image narrower than 0.371Å will still excite an entire CCD element and will therefore appear to be 0.371Å wide. The calculation of resolution must therefore be modified.

CCD Pixel Resolution Diagram

Spectrometer Output

0.06Å

Wavelength

CCD Array Output

0.371 Å

Wavelength

$\Delta\lambda = 0.371$ Å
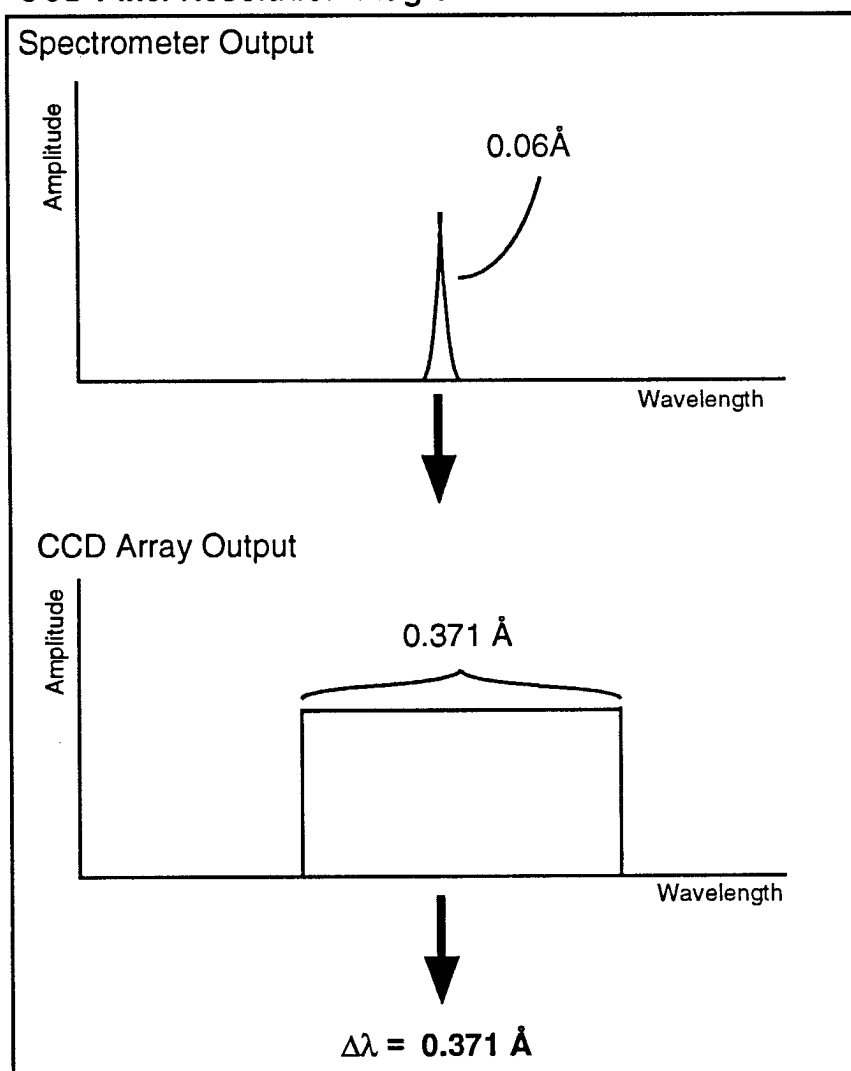
The CCD array limits the minimum image width to 0.371 Å due to its digital nature.

Figure B2

The resolution calculation for the overall sensor suite was therefore modified, substituting the pixel size for the minimum image width value, $\Delta\lambda$.

$$R = \frac{\lambda_0}{\Delta\lambda}$$

$\lambda_0 = 632.8$ nm

$\Delta\lambda = 0.371$ Å

$R = 17,000$

Resolution is a unitless quantity. Finally, it remains to be said that, in spite of the detrimental effects that the digitization of the data had on the resolution, the overall resolution of the sensor suite was nonetheless adequate for this research. As shown in Figure (13), the resolution was fine enough to distinguish the separate modes of the diode laser.